communications in mathematical
match
and in computer chemistry

33 (1996), 169 - 241

Kekulé Count in Tubular Hydrocarbons

Horst Sachs
Technische Universität Ilmenau
Institut für Mathematik
D-98684 Ilmenau

Pierre Hansen
GERAD and École des Hautes Études Commerciales
Montréal, CANADA

Maolin Zheng
GERAD and École des Hautes Études Commerciales
Montréal, CANADA

Abstract

Cylindrical aromatic compounds – carbon cages (fullerenes) and derived hydrocarbons – have become highly interesting objects of chemical research. A *tubulene* (tubular benzenoid) **T** is a hydrocarbon the carbon skeleton of which is a hexagonal system embedded in a cylinder (with its dangling bonds at both ends saturated with hydrogen atoms). The corresponding graph **H** is part of some regular hexagonal tessellation of the cylinder; its perfect matchings represent the possible double-bond arrangements, called Kekulé structures (or patterns), of **T**. It is a well-established rule of thumb that, roughly speaking, the chemical stability of **T** increases with its 'Kekulé count', i.e., with the number K of perfect matchings of **H**.

In this paper, elementary algorithms of low (essentially linear) complexity are presented that allow K to be calculated for an arbitrary tubulene **T**. For some particular classes of tubulenes, recurrence relations and explicit formulae for K are developed and the asymptotic behavior of K is determined. Particularly remarkable is the fact that, in the theory of fully twisted tubulenes, quantities closely related to the Fibonacci numbers play an important role in the results.

1 Introduction

Tubular aromatic carbon structures were first observed by Sumio Iijima [1] in 1991. Since these compounds have attracted attention of chemists, theorists as well as practitioners, because of their remarkable chemical and physical properties which, in particular, seem to indicate that there are vast unexplored areas of future technical application (see, e.g., [1-13]).

In the Kekulé model of a benzenoid molecule M, the system of double bonds is called a *Kekulé structure*. The graph representing the carbon-carbon bonds in M (i.e., the carbon skeleton of M) is a hexagonal system H; each perfect matching of H corresponds to a Kekulé structure of M, and conversely. The number K of Kekulé structures in M (the *Kekulé count*) – i.e., the number of perfect matchings of H – is an interesting parameter: it is an empirically well-established fact that for benzenoid molecules with the same number of hexagons the chemical stability tends to increase with increasing Kekulé count. Therefore, it is a challenging task to investigate tubular (hydro-) carbon structures with respect to the behavior of their Kekulé count. Since, however, the role Kekulé structures play in fullerenes (in the presence of precisely 12 pentagons besides the hexagons) has not yet been clarified, we will consider tubular structures with "open ends", i.e., we will assume that the "dangling bonds" which appear at both ends of the tubule are saturated with hydrogen atoms: thus we will consider only tubular aromatic hydrocarbons (cylindrical benzenoids) which may be termed *tubulenes*. However, the methods developed and results obtained may also shed some light on the interrelations between the chemical stability and the (suitably modified) Kekulé count in fullerene nanotubes.

The Kekulé count itself does not allow molecules with different numbers of hexagons to be compared. Therefore, we define the general graph-theoretical concept of a "perfect matching index" and, applying this index to the skeleton S of an aromatic hydrocarbon molecule M, obtain an index $\kappa(S)$ – called the *Kekulé index* of S, or of M – that meets all natural requirements encountered and thus seems to be the appropriate measure of the density of Kekulé structures in a molecule. Certain variants of this index have already earlier occasionally been considered by chemists [14, 15], but it seems that such a combinatorial parameter has never been profoundly studied.

An important geometric parameter of tubulenes is their *twist*. The methods developed in this paper are applicable to tubulenes of any twist; however, explicit formulae are established only for the extremal cases, namely, for untwisted and fully twisted tubulenes.

It seems that the results allow the tentative statement that in the sense of a general tendency, the Kekulé index increases with increasing twist.

2 The Kekulé index of a graph

2.1 Fundamentals

As usual, $G = (V, E)$ denotes a graph with vertex set V and edge set E.

Let $\mathcal{G}$ be the set of all finite graphs that are allowed to have loops and/or multiple edges. For $G \in \mathcal{G}$, $v = v(G) = |V|$, $e = e(G) = |E|$ and $c = c(G)$ denote the number of vertices, the number of edges and the number of components of G, respectively. Recall that the *cyclomatic number* $z = z(G)$ is the dimension of the cycle space (i.e., the number of linearly independent cycles) of G and that

$$z = e - v + c. \tag{1}$$

Clearly, $z(G) \geq 0$ for every $G \in \mathcal{G}$ and $z(G) = 0$ if and only if G has no circuits, i.e., if and only if G is an (empty or non-empty) forest. Further, if G has components $G_1, G_2, \ldots, G_c$ then

$$z(G) = \sum_{i=1}^{c} z(G_i). \tag{2}$$

A *matching* M of G is a set of pairwise disjoint edges of G. Matching M is called *perfect* if the edges of M cover all vertices of G. Let $m = m(G)$ denote the number of perfect matchings of G. Note that

$$m(G) = \prod_{i=1}^{c} m(G_i). \tag{3}$$

The following lemma is well known and can easily be proved.

Lemma 2.1

$$m(G) \leq 2^{z(G)}. \qquad \square \tag{4}$$

In (4) equality is attained if every component of G is a circuit of even length, but also in other cases, see Fig. 1.

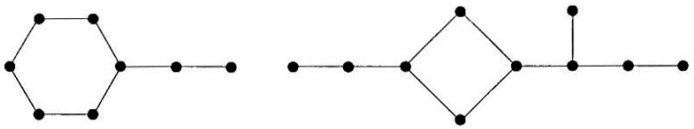

Figure 1.

2.2 The perfect matching index

In order to measure the "density" (more precisely: " logarithmic density") of the set of perfect matchings in a graph G that is not a forest, define the *perfect matching index* $\pi(G)$ by

$$\pi(G) = \frac{\log_2 m(G)}{z(G)} \qquad (G \text{ not a forest}) \tag{5}$$

where, for graphs G that do not have a perfect matching ($m(G) = 0$), the convention $\pi(G) = -\infty$ is adopted.

In what follows we will assume that G is not a forest.

By Lemma 2.1:

Lemma 2.2 $\pi(G) \leq 1.$ □

The following observations may serve to explain why definition (5) of $\pi(G)$ is well motivated.

(*i*) $\pi(G)$ is a normalized "ranking" function which allows graphs of different sizes to be compared. For graphs with the same cyclomatic number, $\pi(G)$ is a monotone function of $m(G)$.

(*ii*) Let G have components $G_1, G_2, \ldots, G_c$. By (2) and (3),

$$\pi(G) = \frac{\sum_{i=1}^{c} \log_2 m(G_i)}{\sum_{i=1}^{c} z(G_i)} = \frac{\sum_{i=1}^{c} z(G_i) \times \pi(G_i)}{\sum_{i=1}^{c} z(G_i)} \tag{6}$$

implying

$$\min_{i=1,2,\ldots,c} \pi(G_i) \leq \pi(G) \leq \max_{i=1,2,\ldots,c} \pi(G_i).$$

In particular, if all G_i have the same perfect matching index then

$$\pi(G) = \pi(G_1).$$

(*iii*) Consider the more general index

$$\pi(q; G) = \frac{\log m(G)}{q(G)}$$

where $q(G) > 0$ satisfies

$$q(G) = \sum_{i=1}^{c} q(G_i)$$

(e.g., $q(G)$ may be chosen to be $v(G), e(G)$ or $c(G)$). All these indices allow statements analogous to (*ii*), and in certain situations it may be more appropriate to use $\pi(v; G), \pi(e; G)$ or $\pi(c; G)$ instead of $\pi(z; G) = \pi(G)$. The reasons why here preference is given to $q(G) = z(G)$ are the following.

(*a*) Perfect matchings have much to do with the cycle structure of G which is (partly) reflected by $z(G)$ (but not by $v(G), e(G)$ or $c(G)$). There is a fundamental inequality relating $m(G)$ to $z(G)$, namely, $\log_2 m(G) \leq z(G)$ (Lemma 2.1).

(*b*) In application to benzenoids B [1], $z(B)$ equals the number h of hexagons (benzene rings) of B, thus $\pi(B)$ is the "logarithmic measure of the Kekulé count per hexagon" which, in a chemical context, sounds reasonable (see [16], p.317). Further, $\pi(B) \leq 1$ where equality holds if and only if B is a single hexagon, i.e., the skeleton of benzene C_6H_6.

(*c*) If sequences of benzenoids (or other plane graphs) of a similar basic structure but with an increasing number of faces (or vertices) are considered then, asymptotically, it makes no difference (up to a constant factor) which of these indices is used; e.g., for all catacondensed [2] benzenoids, $v = 2 + 4h, e = 1 + 5h$, thus, for any increasing sequence of these compounds, $5v \simeq 4e \simeq 20h = 20z$.

[1] A *benzenoid* or *hexagonal system* is a 2-connected finite plane graph whose finite faces are regular hexagons of equal side length. The carbon σ-bond skeleton of an aromatic hydrocarbon is a benzenoid.

[2] A benzenoid is called *catacondensed* if its inner dual is a tree (i.e., if all of its vertices lie on the boundary of the infinite face), otherwise it is called *pericondensed*. In Fig. 2, the L_i and C_i are catacondensed whereas the P_i are pericondensed.

2.3 The Kekulé index

In what follows G will be assumed to be a non-empty connected (c=1) plane graph, not a tree, which has $f = f(G)$ faces (including the infinite face). Combining Euler's formula $v - e + f = 2$ with (1), we obtain

$$z(G) = f(G) - 1. \tag{7}$$

If, in particular, $G = B$ is (the graph of) a benzenoid system with $h = h(B)$ hexagons then $z(G) = h(G)$. In this case, perfect matchings are called "Kekulé structures" or "Kekulé patterns" and their number (the "Kekulé count") is usually denoted by $K(B)$. Therefore, we will call the number

$$\kappa(B) = \pi(B) = \frac{\log_2 K(B)}{h(B)} \tag{8}$$

the *Kekulé index* of the system B.

The index κ (or some variant of it) has been considered by some chemists [14, 15] as a measure of resonance energy per hexagon (or per carbon atom), however it seems that κ has never been profoundly studied: in their book "Kekulé Structures in Benzenoid Hydrocarbons" (1988, [16], p. 317) Cyvin and Gutman say: "... *Especially interesting are the quantities* $(\ln < K >)/h$; *they represent some kind of an average resonance energy per hexagon. ...graphical representations show that these quantities seem to approach limit values when h increases, but nothing has been proved to this effect.*" We will calculate this index (and its limits) for (sequences of) tubular hydrocarbon molecules ("tubulenes"); in these cases, $f(B) - 1 \neq h(B)$, therefore we return to the above (original) definition of $\pi(G)$:

$$\kappa(B) = \pi(B) = \frac{\log_2 K(B)}{f(B) - 1}. \tag{9}$$

For a first comparison, some samples of benzenoids and their Kekulé indices are given in Fig. 2.

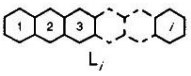

L_i

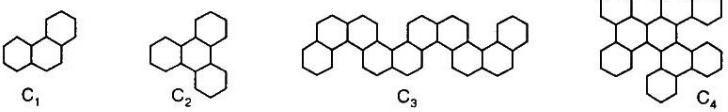

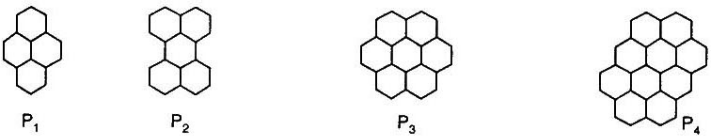

B	h	K	κ
L_1	1	2	1
L_2	2	3	0.79248...
L_3	3	4	$\frac{2}{3} =$ 0.66667...
L_4	4	5	0.58048...
L_7	7	8	$\frac{3}{7} =$ 0.42857...
L_{10}	10	11	0.34594...
L_{15}	15	16	$\frac{4}{15} =$ 0.26667...
L_{31}	31	32	$\frac{5}{31} =$ 0.16129...

B	h	K	κ
C_1	3	5	0.77398...
C_2	4	9	0.79248...
C_3	10	144	0.71699...
C_4	10	189	0.75622...
P_1	4	6	0.64624...
P_2	5	9	0.63399...
P_3	7	20	0.61742...
P_4	10	50	0.56439...

$$\lim_{i \to \infty} \kappa(L_i) = 0$$

Figure 2.

3 Tubular hexagonal systems

3.1 Hexagonal tessellations of the cylinder

A regular hexagonal tessellation of the (surface of the) cylinder C (a cylindrical "graphitic pattern") is a cylindrical tessellation that when C is unwrapped (or rolled) onto the plane – let us say: "printed" on the plane (with unlimited repetitions in both directions) – is turned into the regular hexagonal tessellation (graphite pattern) of the plane. Thus we can study such cylindrical hexagonal tessellations $\mathcal{H}_c$ as parts of the regular hexagonal tessellation $\mathcal{H}$ of the plane, covering a strip between two parallel straight lines a_1, a_2 where points in opposite (orthogonal) position on a_1 and a_2 are to be identified, as indicated in Fig. 3. Note that a_1 and a_2 are consecutive printings of a generator of C, i.e., of a straight line a on C parallel to the axis of C. Let us call this plane representation of $\mathcal{H}_c$ the *natural representation* and denote it by $\mathcal{H}_c^{nat}$.

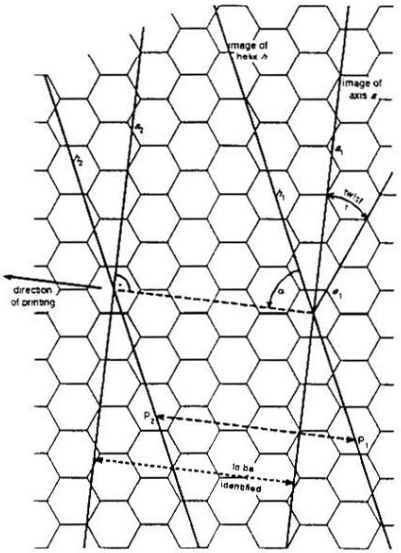

Figure 3.

Sometimes it may be more convenient to replace a with a helix h on C: again a plane image of $\mathcal{H}_c$ is obtained as a part of $\mathcal{H}$ covering a strip between two parallel straight lines h_1, h_2 which are consecutive printings of the helix h; again, h_1 and h_2 are pointwise to be identified, as indicated in Fig. 3.

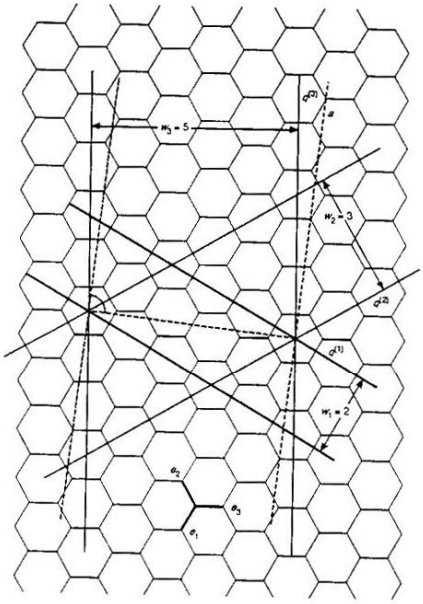

Figure 4.

Let e_1, e_2, e_3 denote the three directions (mod 180^0) of the edges of the hexagons (Fig. 4): then, in particular, the coaxial or helical line on C – we will call it q – can be chosen orthogonal to one of e_1, e_2, e_3; if the axis is not parallel to e_1, e_2 or e_3, then there are three possible choices for q, otherwise there are only two (since, if the axis is parallel to e_i, then the cut on C perpendicular to e_i degenerates into a circle). Thus we obtain three (or two) distinguished representations $\mathcal{H}_c^{(i)}$ of $\mathcal{H}_c$ in the plane such that the hexagons form contiguous columns parallel to the printings of q. Let w_i be the number of these columns in $\mathcal{H}_c^{(i)}$ (i.e., w_i is the "width" of $\mathcal{H}_c^{(i)}$) and choose the labels i such that $w_1 \leq w_2 \leq w_3$ (or $w_1 = w_2$). If the (image of the) axis is

neither parallel nor orthogonal to one of the directions e_1, e_2, e_3 then $w_1 \neq w_2 \neq w_3$; if $w_2 \neq w_3$ then we can choose $\mathcal{H}_c^{(3)}$ (with the largest width) as the *canonical representation* $\mathcal{H}_c^{can}$ of $\mathcal{H}_c$; otherwise, if $w_1 = w_2$, then $\mathcal{H}_c^{(1)}$ and $\mathcal{H}_c^{(2)}$ are congruent and again we have – up to a reflection – a canonical representation $\mathcal{H}_c^{can} = \mathcal{H}_c^{(2)}$ of $\mathcal{H}_c$.

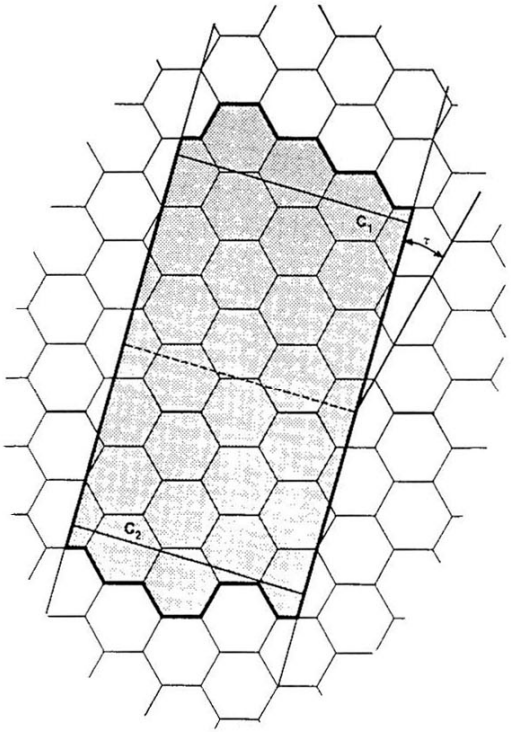

Figure 5.

Note that if the axis is perpendicular to one of the edges of the hexagons then $\mathcal{H}_c^{can}$ coincides with $\mathcal{H}_c^{nat}$. $\mathcal{H}_c$ is considered *untwisted* if the axis is parallel to one of the edges; otherwise, $\mathcal{H}_c$ has an intrinsic *twist* measured by the minimum angle τ of

deviation of the direction of the axis from the directions e_1, e_2, e_3 (Figs. 3, 5, 6; see also Fig. 10: $\tau = min\{\alpha_1, \alpha_2, \alpha_3\}$).

Clearly, τ varies from 0^o (untwisted) to 30^o (fully twisted: the axis is perpendicular to one of e_1, e_2, e_3). Note that τ is in fact a parameter of the *graph* of $\mathcal{H}_c$, not of its particular geometrical realization.

3.2 Tubules

Consider a cylinder C with a cylindrical hexagonal tessellation $\mathcal{H}_c$ on it and perform two distinct cuts perpendicular to the axis of C: these cuts generate on C two distinct circles c_1, c_2 surrounding the axis. Consider the set $\mathcal{S}$ of all hexagons of $\mathcal{H}_c$ that have an interior point lying between c_1 and c_2: these hexagons induce a finite section of $\mathcal{H}_c$ which we will call a *normal tubule* T_N (Fig. 5). Note that (the skeleton of) [3] a normal tubule is a planar bipartite graph which, if drawn on a sphere, has $|\mathcal{S}|$ faces which are hexagons and, corresponding to the "holes" at the ends of T_N, two additional faces F_1, F_2 with even boundary length (in general, $\neq 6$) (Fig. 6).

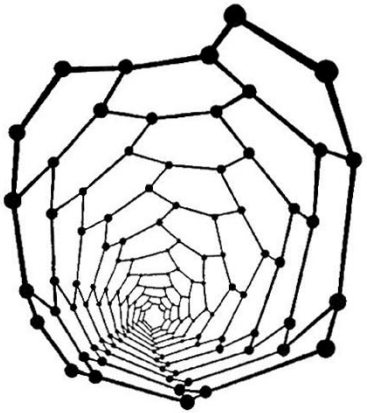

Figure 6a.

[3]For the sake of brevity, we will not distinguish between a tubule and its skeleton.

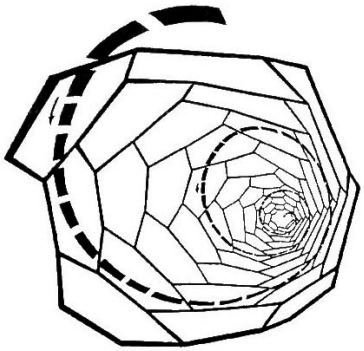

Figure 6b.

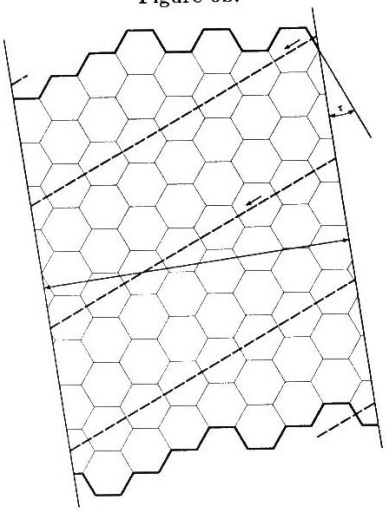

Figure 6c.

A *tubule T in the narrower sense* is a substructure of a normal tubule T_{N_0} such that

- T is connected,
- T has $f-2$ faces which are hexagons generating a tubular surface R (a "ring") surrounding the axis (all of these faces are also faces of T_{N_0}),
- if drawn on the sphere, T is a map which has – in addition to the $f-2$ hexagonal faces mentioned above – two faces F_1, F_2 corresponding to the holes at the ends of R.

There are vertices of valency 2 at both ends of the tubule: it is assumed that in the molecule represented by the tubule dangling bonds are saturated with hydrogen atoms. See Figs. 6, 7.

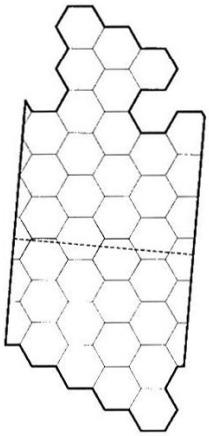

Figure 7a.

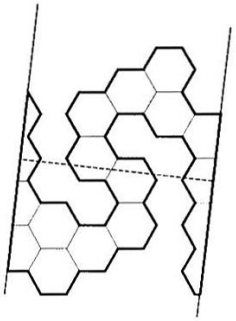

Figure 7b.

Tubules in the wider sense consist of $f-2$ hexagons (as in the narrower sense) and two additional faces F_1, F_2 of a more general shape; we may even allow that, if the surface generated by the hexagons is wrapped around the cylinder, some couples of hexagons overlap (see Fig. 8). In what follows, if no express restriction is made, the word "tubule" and the symbol T are used in their wider sense. For the sake of

brevity, we will also say that a tubule is "embedded" in a tessellation $\mathcal{H}_c$ allowing certain overlaps of a particular kind, as indicated in Fig. 8.

As the cylindrical hexagonal tessellation $\mathcal{H}_c$ in which it is embedded, a tubule T has two particularly distinguished representations: *natural* and *canonical* denoted by T^{nat} and T^{can}, respectively. The *twist* $\tau = \tau(T)$ is that of $\mathcal{H}_c$.

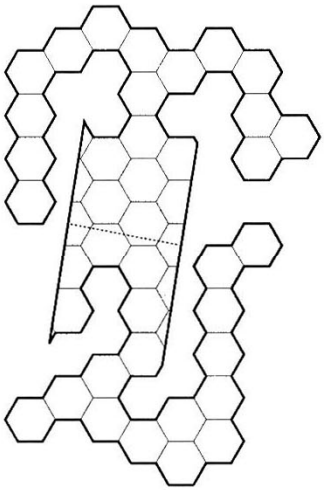

Figure 8.

3.3 Acyclic matchings

Let $G = (V, E)$ and $S \subseteq E$. A circuit of G is called $(S, \bar{S})$ *alternating* iff its edges belong alternatingly to S and $\bar{S} = E - S$. A matching M of G is called *acyclic* iff G contains no $(M, \bar{M})$ alternating circuit.

Consider a regular hexagonal tessellation $\mathcal{H}_c$ of a cylinder and its natural representation $\mathcal{H}_c^{nat}$ in the plane; select an arbitrary edge e of $\mathcal{H}_c^{nat}$, color all edges parallel to e red and all other edges blue: then the red edges form a perfect matching of $\mathcal{H}_c$.

Choosing for e in turn one of the edges e_1, e_2, e_3 incident upon a vertex of $\mathcal{H}_c$, we obtain a partition of the edge set of $\mathcal{H}_c$ into three disjoint perfect matchings M_1, M_2, M_3 (Fig. 9). Assume that the axis a is not parallel to one of the edges e_1, e_2, e_3 and denote the (acute or right) angles between a and e_i by α_i (Fig. 10): precisely one of these angles – say, α_3 – exceeds 60^o. Then matchings M_1 and M_2 are acyclic whereas M_3 is not. This is easily seen from Fig. 10: select an arbitrary vertex A: the figure shows that A does not lie on any $(M_1, \bar{M}_1)$ or $(M_2, \bar{M}_2)$ alternating circuit, whereas A does lie on $(M_3, \bar{M}_3)$ alternating circuits (e.g., circuit C of Fig 10). If, however, the axis is parallel to one of the edges e_i – to e_1, say – then $\alpha_1 = 0, \alpha_2 = \alpha_3 = 60^o$: then matching M_1 is acyclic whereas M_2 and M_3 are not. In any case, at least one (in general two) among M_1, M_2, M_3 is (are) acyclic.

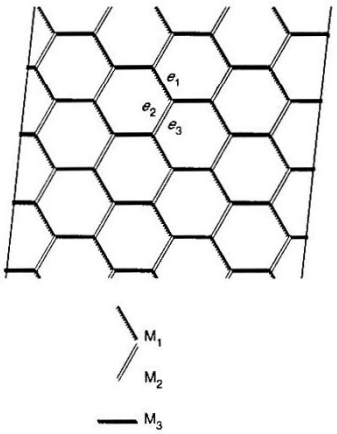

Figure 9.

Let M be one of these acyclic perfect matchings of $\mathcal{H}_c$. Then the restriction $M|_T$ of M with respect to any tubule T embedded in $\mathcal{H}_c$ is an acyclic matching of T. Direct the axis of $\mathcal{H}_c$ vertically thus distinguishing for every edge of M an upper and a lower end vertex; color the edges of $\bar{M}$ blue, the edges of M red, their upper end vertices black and their lower end vertices white (Fig. 11); clearly, every edge of $\mathcal{H}_c$ connects a black to a white vertex.

Direct the red edges from black to white and the blue edges from white to black. Let Ω denote the orientation of $\mathcal{H}_c$ so obtained and let $\mathcal{H}_c^{\Omega}, T^{\Omega}$ be the directed graphs corresponding to $\mathcal{H}_c$ and T, respectively. The sources (sinks) of T^{Ω} are called its *peaks* (*valleys*); all peaks (valleys) are white (black). The sources and sinks are precisely those vertices which are not incident upon a red edge.

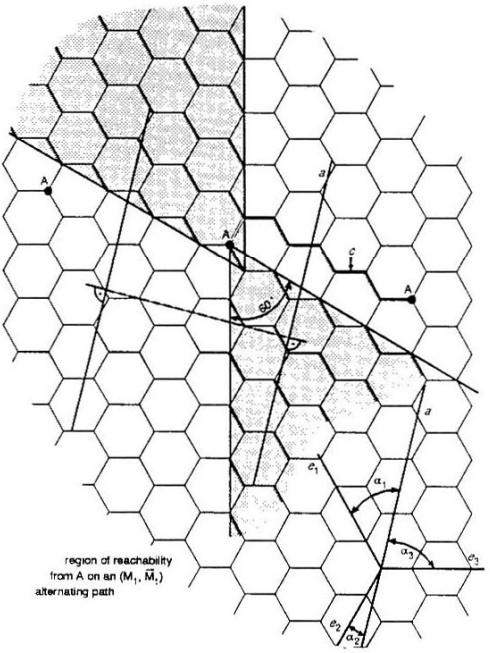

Figure 10.

As in the case of plane benzenoid systems (see, e.g., [17]), the following propositions hold.

(I) *If T has a Kekulé structure then T^{Ω} has as many sources as sinks.*

(II) *There is a* (1,1) *correspondence between the set of Kekulé structures of* T *and the set of systems of disjoint directed paths in* T^{Ω} *connecting the sources with the sinks such that in each source commences, and in each sink terminates, exactly one path of the system; if the axis is brought into perpendicular position (as assumed above) then, on each of these paths, the heights of the white vertices and the heights of the black vertices form strictly decreasing monotone sequences.*

3.4 Kasteleyn orientations

We need the concept of a Kasteleyn orientation of a plane graph; such orientations were first used by P.W. Kasteleyn ([18] (1961), [19] (1967)) in his pioneering work on counting dimer coverings of sections of the square lattice.

Let G be an embedding of a connected planar graph in the plane (or in the sphere) and suppose that G is equipped with some orientation ω of its edges; let F be a face of G. The orientation ω is said to be *Kasteleyn with respect to* F iff the number of edges of the boundary of F whose left bank belongs to F is odd; ω is called a *Kasteleyn orientation* of G iff ω is Kasteleyn with respect to all faces (including the infinite face) of G.

Clearly, the orientation Ω of $\mathcal{H}_c^{\Omega}$ is Kasteleyn, and the orientation $\Omega|_T$ (i.e., the orientation of T^{Ω}) is Kasteleyn with respect to every hexagonal face of T (see Fig. 11).

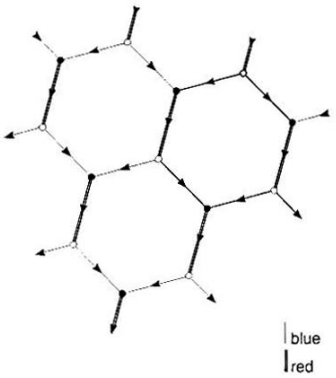

Figure 11.

Let $\mu = \Omega|_T$. Two cases arise:
(i) μ is Kasteleyn with respect to F_1.

Then, necessarily, μ is Kasteleyn with respect to F_2, too: thus μ is a Kasteleyn orientation of T. Let $\mathcal{K} = \mu$ and sgn (x, y)=sgn (e)=1 for every edge $e = (x, y)$ of T.

(ii) μ is not Kasteleyn with respect to F_1.

Then we obtain a Kasteleyn orientation $\mathcal{K}$ from μ in the following way. We draw a smooth curve t (a transversal) from some point in the interior of F_1 to some point in the interior of F_2 that meets no vertex, touches no edge, intersects no edge more than once, and passes no face more than once; then we change the direction of all edges intersected by t. We indicate this change by assigning minus signs to all edges intersected by t: so every edge $e = (x, y)$ obtains a weight, namely:

$$\text{sgn}(x, y) = \text{sgn}(e) = \begin{cases} -1 & \text{if } e \text{ is intersected by } t \\ +1 & \text{otherwise.} \end{cases}$$

Clearly, the new orientation $\mathcal{K}$ is Kasteleyn (Fig. 12).

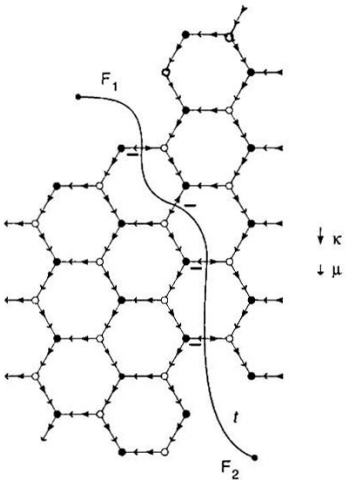

Figure 12.

4 Calculating the number of Kekulé structures

4.1 The algorithm: general case

Having orientations μ and $\mathcal{K}$, we can now apply algorithm $\mathcal{A}$ of [21] (see also [20, 22]) for calculating the number $K(T)$ of Kekulé structures of tubule T.

The algorithm runs as follows. First check whether the number p of peaks of T equals the number v of valleys: if not then T does not have Kekulé structures and $K(T) = 0$. Therefore suppose that $p = v$. Label the peaks, and also the valleys, in an arbitrary way from 1 through p. Let $\{P_1, P_2, \ldots, P_p\}$ and $\{V_1, V_2, \ldots, V_p\}$ be the set of peaks and the set of valleys, respectively. Let

$$\mathbf{q}(P_k) = (\delta_{k1}, \delta_{k2}, \ldots, \delta_{kp}) \quad (\delta_{ii} = 1, \delta_{ij} = 0 \ \ if\ i \neq j), k = 1, 2, \ldots, p.$$

Following the arrows of orientation μ, calculate for every vertex x of T that is not a peak the vector

$$\mathbf{q}(x) = \sum \mathrm{sgn}(x', x) \times \mathbf{q}(x') \tag{10}$$

where the sum is taken over all (i.e., over the one or two) predecessors x' of x.

For valley V_i, let

$$\mathbf{q}(V_i) = (q_{i1}, q_{i2}, \ldots, q_{ip}) \quad (i = 1, 2, \ldots, p)$$

and form the $p \times p$ matrix

$$Q = \begin{pmatrix} \mathbf{q}(V_1) \\ \vdots \\ \mathbf{q}(V_p) \end{pmatrix} = (q_{ik})_{i,k=1,2,\ldots,p}.$$

Then

$$K(T) = |detQ| = abs|q_{ik}|. \tag{11}$$

Remark. Once we have chosen the orientation μ, it does not matter which representation of $T - T^{nat}, T^{can}$ or any other representation – we use for carrying out the above algorithm: any one will do. Thus we are free to choose that representation which seems to be the most convenient for the purpose.

For some examples see Figs. 13–15. Note that Figs. 13 a, b represent the same tubule.

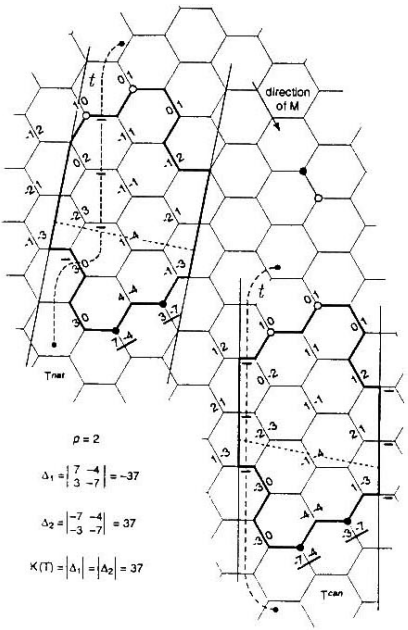
direction of M
t
t
Tnat
Tcan
p = 2
$\Delta_1 = \begin{vmatrix} 7 & -4 \\ 3 & -7 \end{vmatrix} = -37$
$\Delta_2 = \begin{vmatrix} -7 & -4 \\ -3 & -7 \end{vmatrix} = 37$
$K(T) = |\Delta_1| = |\Delta_2| = 37$

Figure 13a.

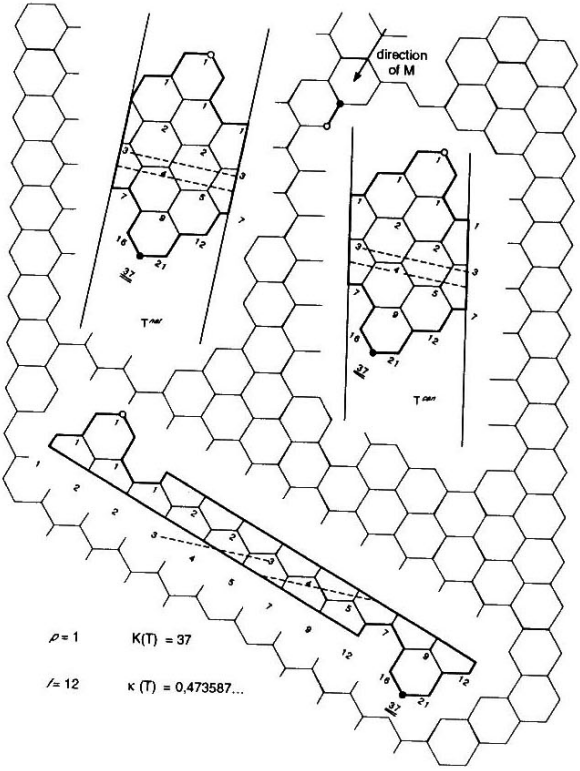

Figure 13b.

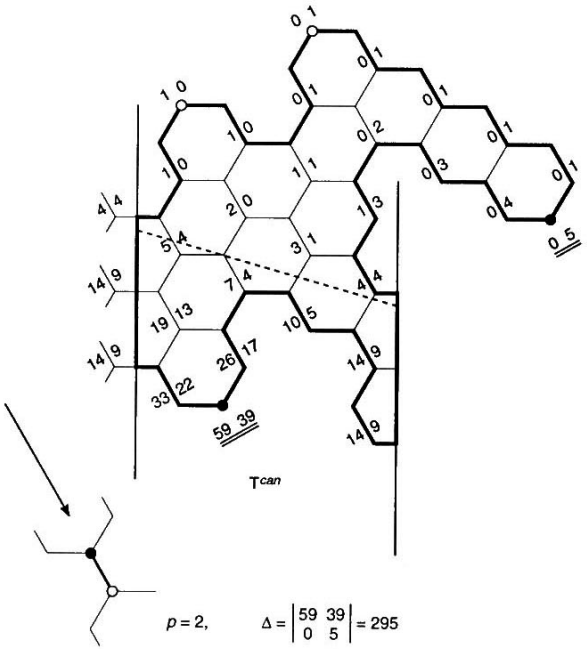

Figure 14.

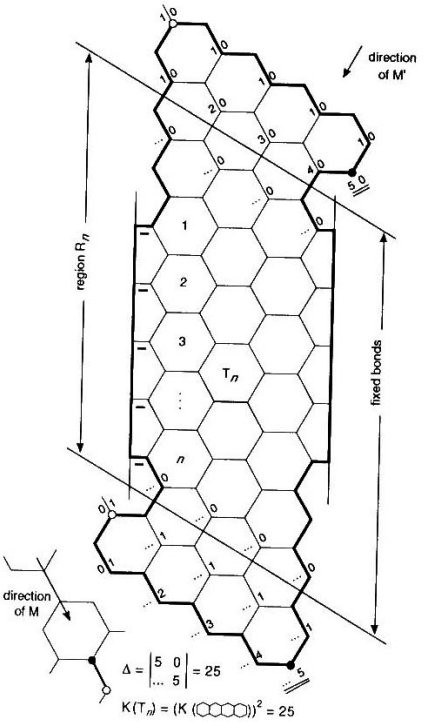
direction
of M'
region R_n
fixed bonds
1
2
3
T_n
n
direction
of M
$\Delta = \begin{vmatrix} 5 & 0 \\ \dots & 5 \end{vmatrix} = 25$
$K(T_n) = (K(\bigcirc\!\!\bigcirc\!\!\bigcirc\!\!\bigcirc\!\!\bigcirc))^2 = 25$

Figure 15.

4.2 The untwisted normal tubule (Fig.16)

Here the situation is simple, almost trivial. Let $\mathcal{N}_0$ denote the class of all normal tubules with $\tau = 0°$. The edge set E of a tubule $T \in \mathcal{N}_0$ consists of the class E' of all edges parallel to the axis and the class $E'' = E - E'$ of all edges forming "sawtooth rings" surrounding the axis. Two consecutive sawtooth rings define a layer of hexagons forming a closed tape around the cylinder. Let l be the number of these layers (l measures the height – or length – of T) and let p denote the number of peaks of T (Fig. 16: p is the number of hexagons in one layer and measures the circumference of T). Clearly, l and p are the only two parameters of the class $\mathcal{N}_0$, their product $l \times p$ equals the number $h = f - 2$ of hexagons of $T = T(l, p)$.

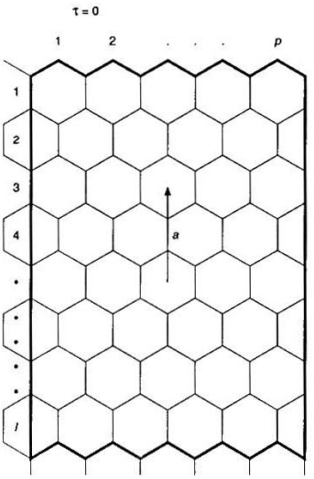

Figure 16.

It is easy to see that no edge of E' can be an element of any perfect matching of T (if T is considered the skeleton of a tubular hydrocarbon then, in Kekulé's model, the edges of E' represent fixed single bonds). Omitting these edges from T, we obtain $l + 1$ disjoint circuits (the sawtooth rings) each of length $2p$. Each of these circuits having exactly 2 perfect matchings, the total number of perfect matchings of T is

$$K(T(l,p)) = 2^{l+1}$$

(note that K does not depend on p). This immediately yields

$$\begin{aligned} \kappa(T(l,p)) &= \frac{l+1}{lp+1}, \\ \lim_{l\to\infty} \kappa(T(l,p)) &= 1/p, \\ \lim_{p\to\infty} \kappa(T(l,p)) &= 0. \end{aligned}$$

These results show that – except for some extremely small tubules of little chemical interest – the Kekulé index of untwisted normal tubules is small; in particular,

$$\text{if } (p-4)l > 3 \text{ then } \kappa(T(l,p)) < \frac{1}{4}.$$

4.3 The fully twisted tubule

4.3.1 Preliminaries

The next task could be the investigation of untwisted *non*-normal tubules: such an investigation can indeed be carried out, but we will skip it here and turn our attention to the (chemically probably more important) case of the fully twisted tubule; having solved this case we will find it much easier to deal with the general case of an arbitrarily twisted tubule.

Consider the fully twisted hexagonal cylindrical tessellation $\tilde{\mathcal{H}}_c$ and its plane image $\tilde{\mathcal{H}}_c^{nat} = \tilde{\mathcal{H}}_c^{can}$ (Fig. 17). Here we have two choices for the acyclic matching M where one is obtained from the other by a reflection with respect to the direction of the axis. Without loss of generality, let us suppose that we have chosen M as in Fig. 17. The number of columns of contiguous hexagons parallel to the axis is necessarily even, say $2q$; this number measures the circumference c of $\tilde{\mathcal{H}}_c$.

4.3.2 Coordinates

We introduce coordinates k, n for the horizontal edges g as indicated in Fig. 17; k is to be taken modulo q (whenever convenient, we shall assume $0 \le k \le q-1$). The black

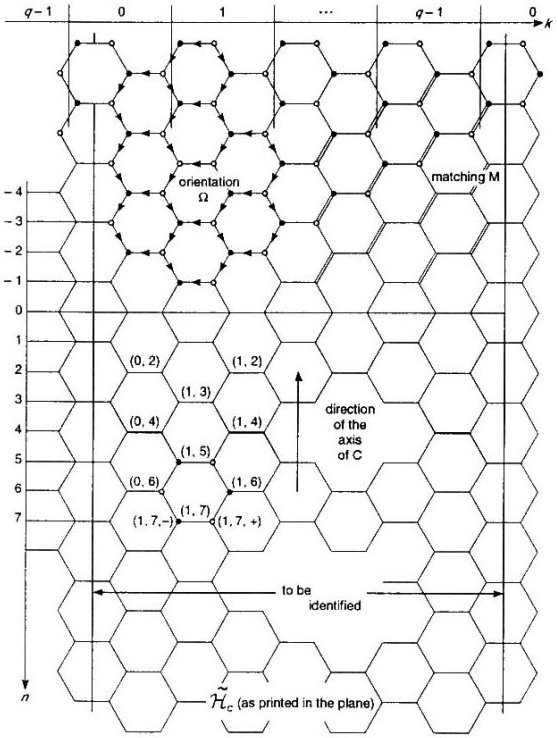
q − 1
0
1
···
q − 1
0
k
orientation
Ω
matching M
−4
−3
−2
−1
0
1
2
3
4
5
6
7
n
(0, 2)
(1, 2)
(1, 3)
(0, 4)
(1, 4)
(1, 5)
(0, 6)
(1, 6)
(1, 7)
(1, 7, −)
(1, 7, +)
direction
of the
axis
of C
to be
identified
$\tilde{\mathcal{H}}_c$ (as printed in the plane)

Figure 17.

vertex B and the white vertex W connected by g are given the coordinates $(k, n, -)$ and $(k, n, +)$, respectively. We shall briefly write $g = (k, n), B = (k, n, -), W = (k, n, +)$ (Fig. 18).

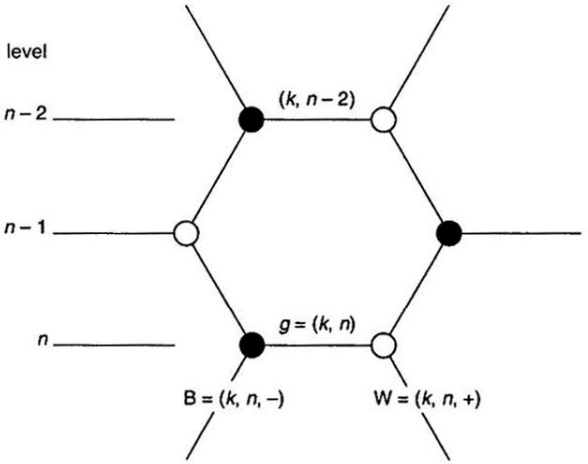

Figure 18.

4.3.3 Normal subtubules

We will now assume that the tubule T considered is part of $\tilde{\mathcal{H}}_c$ and contains a normal subtubule T_m which occupies levels $n = 0$ through $n = m$ (Fig. 19). Note that T_m covers $(m-1)q$ hexagons; therefore, it is reasonable to define the *height* (or *length*) l of T_m to be equal to $(m-1)/2$ (which need not be an integer): then the number of hexagons of T_m is

$$h = (m-1) \times q = l \times c = \text{height} \times \text{ circumference.}$$

We can now calculate $K(T)$ by applying algorithm $\mathcal{A}$ to T in the following way.

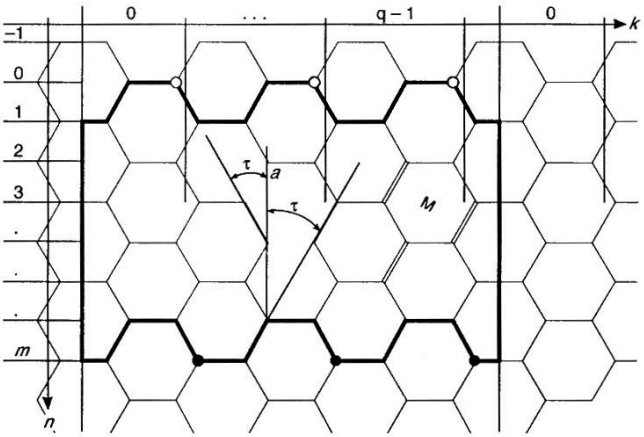

Figure 19.

Step 1. We start from the peaks of T and calculate vectors $\mathbf{q}(x)$ as described in Section 4.1 until we reach the "upper end" of subtubule T_m, i.e., we calculate $\mathbf{q}(x)$ for the white vertices x^* on levels -1 and 0 of tubule T_m.

Step 2. We continue with algorithm $\mathcal{A}$ using the components of the vectors $\mathbf{q}(x^*)$ as the initial values for the recurrence procedure (formula (10)) to calculate vectors $\mathbf{q}(y^*)$ for the white vertices y^* on levels m and $m+1$, i.e., on the "lower end" of tubule T_m.

Step 3. We continue the calculation and eventually obtain the vectors $\mathbf{q}(V)$ for the valleys V of T. $K(T)$ is now given by formula (11).

As we are interested in the behavior of $K(T)$ for increasing values of m, we will study Step 2 separately. If in particular T is itself a normal tubule, i.e., if $T = T_m$ for some m, then we need only insert the special 0,1 initial values and stop at level $m+1$.

For the given tubule T, the orientation μ may or may not be Kasteleyn; therefore, we have to distinguish two cases (see Section 3.4).

Case A: *μ is Kasteleyn.* Then $\operatorname{sgn}(e) = 1$ for all edges e of $\tilde{\mathcal{H}}_c$.

Case B: *μ is not Kasteleyn.* Then we choose for the transversal t (a suitable section of) a straight line perpendicular to the edges $(0, n)$, i.e., we let

$$\mathrm{sgn}(e) = \begin{cases} -1 & \text{if } e = (0, n), \quad n = 0, \pm 1, \pm 2, \ldots \\ 1 & \text{otherwise} \end{cases}$$

for all edges e of $\tilde{\mathcal{H}}_c$.

4.3.4 The general recurrence procedure

For carrying out Step 2 (Section 4.3.3) in its general form, we start from recurrence (10) (Section 4.1) and write it down componentwise for $\tilde{\mathcal{H}}_c$. Let $q_i(x)$ be one of the components of the vector $\mathbf{q}(x)$: we fix i and , using the values $q_i(x^*)$ for the white vertices on levels -1 and 0 (see Step 1) as the initial values for Step 2, intend to calculate the values $q_i(x)$ for the vertices x on level n where n is an integer variable (n replaces m in the formulation of Step 2). Let vertex x have coodinates k, n, s ($s \in \{-1, +1\}$) (Section 4.3.2). To avoid unnecessary subscripts, set

$$q_i(x) = \varphi(x) = \varphi(k, n, s).$$

The initial values $q_i(x^*)$ (see above) are to be considered arbitrary: therefore, for $x^* = (k, 0, +)$ and $x^{**} = (k, -1, +)$ we set

$$q_i(x^*) = \varphi(k, 0, +) = a_k$$

and

$$q_i(x^{**}) = \varphi(k, -1, +) = b_k,$$

respectively, where a_k and b_k are unspecified variables. The task we have to solve is the following.

Given $\tilde{\mathcal{H}}_c$ with circumference $2q$ equipped with coordinates k, n (see Section 4.3.2),

define the function

$$\varphi(k, n, s) \quad (k \bmod q;\ n = 0, \pm 1, \pm 2, \ldots;\ s \in \{+1, -1\})$$

for all vertices (k, n, s) of $\tilde{\mathcal{H}}_c$ by the recursion formulae

$$\varphi(k, n+2, +) = \begin{cases} \varphi(k, n+1, -) & = \varphi(k, n, +) + \varphi(k, n+1, +) \\ & \quad \text{if } n \text{ is odd} \\ \varphi(k+1, n+1, -) & = \varphi(k, n, +) \\ & \quad +\sigma_{k+1}\varphi(k+1, n+1, +) \\ & \quad \text{if } n \text{ is even} \end{cases} \tag{12}$$

and the initial values

$$\begin{cases} \varphi(k, 0, +) & = a_k \\ \varphi(k, -1, +) & = b_k \end{cases} \quad (k \bmod q) \tag{13}$$

where in case A:

$$\sigma_k = 1 \quad \text{for all } k \bmod q$$

and in case B:

$$\sigma_k = \begin{cases} -1 & \text{if } k \equiv 0 \bmod q \\ 1 & \text{otherwise,} \end{cases}$$

calculate $\varphi(k, n, s)$.

As $\varphi(k, n, -)$ can be eliminated from the definition of $\varphi(k, n, +)$, we will briefly write

$$\varphi(k, n) = \varphi(k, n, +);$$

drawing figures, it is convenient to suppress $\varphi(k, n, -)$ and to write the value of $\varphi(k, n)$ just above the edge (k, n), i.e., left to the white vertex $(k, n, +)$ (Fig. 18).

For $\varphi(k, n)$, the defining equations (12) and (13) reduce to

$$\varphi(k, n+2) = \begin{cases} \varphi(k, n) + \varphi(k, n+1) & \text{if } n \text{ is odd} \\ \varphi(k, n) + \sigma_{k+1}\varphi(k+1, n+1) & \text{if } n \text{ is even,} \end{cases} \tag{12'}$$

$$\begin{cases} \varphi(k, 0) & = a_k \\ \varphi(k, -1) & = b_k. \end{cases} \tag{13'}$$

Let

$$\begin{cases} a_{k,m} = \varphi(k, 2m) \\ b_{k,m} = \varphi(k, 2m+1) \end{cases} \tag{14}$$

(thus $a_{k,0} = a_k, b_{k,-1} = b_k$).
By (12'),

$$\begin{cases} a_{k,m+1} = a_{k,m} + \sigma_{k+1} b_{k+1,m} \\ b_{k,m+1} = a_{k,m+1} + b_{k,m} \end{cases} \tag{15}$$

equivalent to

$$\begin{cases} \triangle a_{k,m} = \sigma_{k+1} b_{k+1,m} \\ \triangle b_{k,m} = a_{k,m+1} \end{cases} \tag{16}$$

where $\triangle$ denotes the difference operator ($\triangle f(m) = f(m+1) - f(m)$) with respect to m (k is kept fixed).

Applying $\triangle$ a second time, we have

$$\begin{cases} \triangle^2 a_{k,m} = \sigma_{k+1} \triangle b_{k+1,m} = \sigma_{k+1} a_{k+1,m+1} \\ \triangle^2 b_{k,m} = \triangle a_{k,m+1} = \sigma_{k+1} b_{k+1,m+1}. \end{cases} \tag{17}$$

Repeating $\triangle^2$ q times, we obtain

$$\begin{cases} \triangle^{2q} a_{k,m} = \sigma_k^* a_{k+q,m+q} = \sigma_k^* a_{k,m+q} \\ \triangle^{2q} b_{k,m} = \sigma_k^* b_{k+q,m+q} = \sigma_k^* b_{k,m+q} \end{cases} \tag{18}$$

where

$$\sigma_k^* = \sigma_{k+1} \sigma_{k+2} \dots \sigma_{k+q} = \begin{cases} 1 & \text{in case A} \\ -1 & \text{in case B.} \end{cases}$$

The characteristic equation for both difference equations (18) is the same, namely

$$(x-1)^{2q} = \delta x^q \tag{19}$$

where

$$\delta = \begin{cases} 1 & \text{in case A} \\ -1 & \text{in case B.} \end{cases}$$

Equation (19) is equivalent to the set of equations

$$(x-1)^2 = \epsilon(q,j)x, \quad j \in \{0,1,\ldots,q-1\} \tag{20}$$

where

$$\epsilon(q,j) = \begin{cases} e^{\frac{2j}{q}\pi i} & \text{in case A} \\ e^{\frac{2j+1}{q}\pi i} & \text{in case B.} \end{cases}$$

For fixed q, we abbreviate

$$\epsilon = e^{\frac{\pi}{q}i}, \quad \epsilon_j = \epsilon(q,j) = \begin{cases} \epsilon^{2j} & \text{in case A} \\ \epsilon^{2j+1} & \text{in case B;} \end{cases}$$

note that ϵ is a primitive $2q$-th root of unity.

Let s denote the sign: $s \in \{+1,-1\}$. If s is used without comment, then both signs are to be applied. The roots of equation (19) – obtained via (20) – are

$$\begin{aligned} x_{js} &= \tfrac{1}{2}\{2+\epsilon_j + s\sqrt{\epsilon_j(4+\epsilon_j)}\}, \\ & j = 0,1,\ldots,q-1;\ s = +1,-1. \end{aligned} \tag{21}$$

Recall: The square root of a complex number $x+iy$ is made unique by the following convention:
if $(u+iv)^2 = x+iy$ then

$$\sqrt{x+iy} = u^* + iv^* = \begin{cases} \operatorname{sgn}(u)(u+iv) & \text{if } u \neq 0 \\ i|v| & \text{if } u = 0; \end{cases}$$

if $y \neq 0$ then

$$\begin{cases} u^* = \dfrac{1}{\sqrt{2}}\sqrt{\sqrt{x^2+y^2}+x} & > 0 \\ v^* = \dfrac{\operatorname{sgn}(y)}{\sqrt{2}}\sqrt{\sqrt{x^2+y^2}-x}. \end{cases} \tag{22}$$

Abbreviating $r_j = \sqrt{\epsilon_j(4+\epsilon_j)}$ we have

$$x_{js} = \tfrac{1}{2}\{2+\epsilon_j + sr_j\}. \tag{21'}$$

Let

$$y_{js} = x_{js} - 1 = \tfrac{1}{2}\{\epsilon_j + sr_j\}.$$

y_{j+} and y_{j-} are the roots of the equation

$$y^2 = \epsilon_j(y+1) \tag{23}$$

from which we obtain

$$y_{js}^2 = \epsilon_j x_{js}, \quad x_{js} = y_{js} + 1 = \epsilon_j^{-1} y_{js}^2. \tag{24}$$

By (19) (or 23), the y_{js} $(j = 0, 1, \ldots, q-1; s = +1, -1)$ are the roots of the equation

$$y^{2q} = \delta(y+1)^q. \tag{25}$$

Define

$$\eta_j = \eta(q,j) = \begin{cases} e^{\frac{j}{q}\pi i} & \text{in case A} \\ e^{\frac{2j+1}{2q}\pi i} & \text{in case B} \end{cases} \tag{26}$$

and

$$z_{js} = \eta_j^{-1} y_{js}.$$

Clearly,

$$\eta_j^2 = \epsilon_j, \tag{27}$$

thus by (24),

$$x_{js} = z_{js}^2. \tag{28}$$

Note that

$$z_{js}^2 - 1 = x_{js} - 1 = y_{js} = \eta_j z_{js}. \tag{29}$$

Let us abbreviate

$$\sum_{j=1}^{q} \sum_{s\in\{+1,-1\}} f(j,s) \quad \text{as} \quad \sum_{j,s} f(j,s).$$

$a_{k,m}$ and $b_{k,m}$ being solutions of difference equation (18) whose characteristic equation (19) has the pairwise distinct roots x_{js}, they can now be expressed in the form

$$\begin{cases} a_{k,m} = \sum_{j,s} \tilde{A}^s_{kj} x^m_{js} = \sum_{j,s} A^s_{kj} z^{2m+1}_{js}, \\ b_{k,m} = \sum_{j,s} \tilde{B}^s_{kj} x^m_{js} = \sum_{j,s} B^s_{kj} z^{2m+2}_{js} \end{cases} \tag{30}$$

where $A^s_{kj} = \tilde{A}^s_{kj} z^{-1}_{js}$, $B^s_{kj} = \tilde{B}^s_{kj} z^{-2}_{js}$.

Inserting these expressions into (16) and using (29), we obtain

$$\begin{aligned} \sum_{j,s} B^s_{k+1,j} z^{2m+2}_{js} &= b_{k+1,m} = \sigma_{k+1} \triangle a_{k,m} \\ &= \sigma_{k+1} \sum_{j,s} A^s_{kj} z^{2m+1}_{js} (z^2_{js} - 1) \\ &= \sum_{j,s} \sigma_{k+1} A^s_{kj} \eta_j z^{2m+2}_{js}, \end{aligned}$$

$$\begin{aligned} \sum_{j,s} A^s_{kj} z^{2m+3}_{js} &= a_{k,m+1} = \triangle b_{k,m} \\ &= \sum_{j,s} B^s_{kj} z^{2m+2}_{js} (z^2_{js} - 1) \\ &= \sum_{j,s} B^s_{kj} \eta_j z^{2m+3}_{js}. \end{aligned}$$

Equating the coefficients of equal power terms (which is legal since the z_{js} are pairwise distinct implying that the corresponding Vandermonde determinant is non-zero) we see that

$$B^s_{k+1,j} = \sigma_{k+1} A^s_{kj} \eta_j, \tag{31a}$$

$$A^s_{kj} = B^s_{kj} \eta_j. \tag{31b}$$

Inserting $B^s_{k+1,j}$ from (31a) into (31b), we obtain

$$A^s_{k+1,j} = B^s_{k+1,j} \eta_j = \sigma_{k+1} \eta^2_j A^s_{kj},$$

thus, by (27),

$$A^s_{k+1,j} = \sigma_{k+1}\epsilon_j A^s_{kj}. \tag{32a}$$

In the same way, the insertion of A^s_{kj} from (31b) into (31a) yields

$$B^s_{k+1,j} = \sigma_{k+1}\epsilon_j B^s_{kj}. \tag{32b}$$

To put it more briefly, let C stand for A or B: then, simply,

$$C^s_{k+1,j} = \sigma_{k+1}\epsilon_j C^s_{kj}. \tag{32c}$$

Iterating (32c) we obtain

$$C^s_{kj} = \sigma_k\sigma_{k-1}\ldots\sigma_1\epsilon_j^k C^s_{0j}. \tag{33}$$

In **case A**, (33) reduces to

$$C^s_{kj} = \epsilon_j^k C^s_{0j} = e^{\frac{jk}{q}2\pi i} C^s_{0j}. \tag{33A}$$

Summation over k gives

$$\begin{aligned} \sum_{k=0}^{q-1} C^s_{kj} &= C^s_{0j}\sum_{k=0}^{q-1} e^{\frac{jk}{q}2\pi i} \\ &= \begin{cases} qC^s_{00} & \text{if } j \equiv 0 \pmod q \\ 0 & \text{otherwise.} \end{cases} \end{aligned} \tag{34A}$$

For $j \equiv 0 \pmod q$ we obtain from (33A)

$$C^s_{00} = C^s_{10} = \ldots = C^s_{q-1,0}. \tag{35A}$$

Note that these numbers are the coefficients of the powers of the only two real roots of (25) (case A), namely,

$$z_{0s} = y_{0s} = \tfrac{1}{2}\{1 + s\sqrt{5}\}.$$

In **case B**, in (33) the factor

$$\epsilon_j^k = e^{\frac{2j+1}{q}k\pi i}$$

has, as a function of k, the period $2q$; note that $\epsilon_j^{k+q} = -\epsilon_j^k$; thus the factor $\sigma_k\sigma_{k-1}\ldots\sigma_1\epsilon_j^k$ has indeed the period q – as required.

Restricting k to the interval $[0,1,\ldots,q-1]$, we obtain from (33) in both cases

$$C_{kj}^s = \epsilon_j^k C_{0j}^s, \quad k = 0,1,\ldots,q-1. \tag{33'}$$

Equations (31b) and (33') allow the $4q^2$ coefficients A_{kj}^s, B_{kj}^s to be expressed by the $2q$ coefficients A_{0j}^s:

$$\begin{cases} A_{kj}^s = \epsilon_j^k A_{0j}^s, \\ B_{kj}^s = \epsilon_j^k B_{0j}^s = \eta_j^{-1}\epsilon_j^k A_{0j}^s, \quad k = 0,1,\ldots,q-1. \end{cases} \tag{36}$$

In order to calculate the $2q$ coefficients A_{0j}^s we start from the $2q$ initial values (13):

$$\begin{aligned} a_{k,0} &= \varphi(k,0) = a_k, \\ b_{k,-1} &= \varphi(k,-1) = b_k \quad (k = 0,1,\ldots,q-1) \end{aligned}$$

and calculate $2q$ consecutive values $a_{0,m_0+\mu}$ $(\mu = 0,1,\ldots,2q-1)$. This can be done in many ways; the number of additions to be performed is minimum if we use also sites with negative ordinate n and proceed as indicated in Fig. 20 (without surrounding the cylinder): the least number of additions to be executed is

$$1+2+3+\ldots+(2p-1) = p(2p-1).$$

The coefficients A_{0j}^s are then found by solving the $2q$ linear equations

$$\sum_{j,s} z_{js}^{2(m_0+\mu)+1} A_{0j}^s = a_{0,m_0+\mu}, \quad \mu = 0,1,\ldots,2q-1 \tag{37}$$

(see equations (30)).

4.3.5 A first general result

Consider a fully twisted tubule T_1^* which has as many valleys as peaks $= p^*$, say – and contains a normal tubule T_1 of height l_1 as a subtubule. We may, without loss

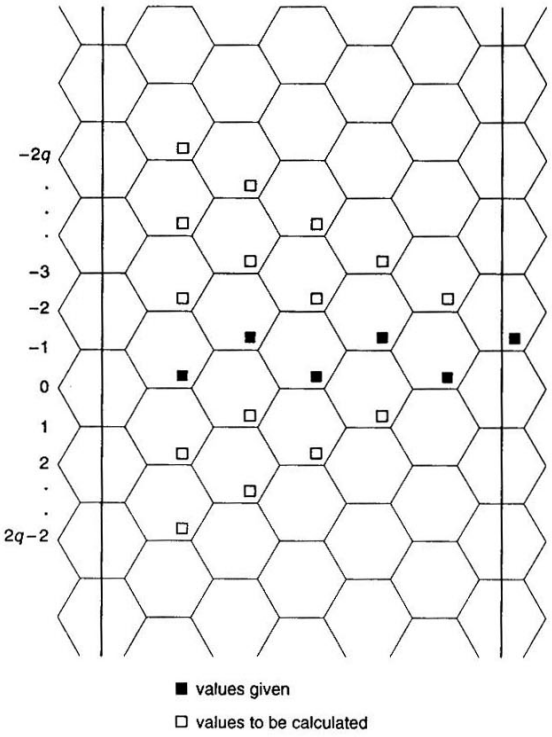

Figure 20.

of generality, assume that $l_1 = 0$: then T_1 covers only levels $n = 0$ and $n = 1$, it degenerates to a circuit surrounding the cylinder.

Let T_n^* $(n \geq 1)$ denote the tubule which is obtained from T_1^* by replacing T_1 with a normal tubule T_n of height $\frac{1}{2}(n-1)$, and let $K_n = K(T_n^*)$. To keep the situation transparent, we will proceed in double steps, i.e., we assume that n runs through the odd integers only: $n = 2m+1$, $m = 0, 1, 2, \ldots$. We may calculate K_n as described in Section 4.3.3. At the end of Step 2 we have obtained vectors $\mathbf{q}(y^*)$ with the property that all their components have the form $\sum_{j,s} c_{js} x_{js}^m$ where the x_{js} are the $2q$ roots of equation (19) and the c_{js} do not depend on m (see equations (30)). The same applies to the components of the vectors $\mathbf{q}(V)$ that we obtain at the end of Step 3 and, therefore, also to all entries of the matrix Q_n^* of size $p^* \times p^*$ formed by these vectors. Let $D_m = det\ Q_{2m+1}^*$. According to equation (11),

$$K_{2m+1} = |D_m|.$$

Note that $D_m = \sum_{i=1}^{R} d_i u_i^m$ where u_i runs through all $R = \binom{2q+p^*-1}{p^*}$ possible products formed by p^* factors x_{js} (repetitions allowed) and the coefficients d_i do not depend on m.

Suppose that $u_1, u_2, \ldots, u_N$ are those of the u_i that satisfy $d_i \neq 0$. Let

$$\prod_{i=1}^{N}(u - u_i) = u^N - a_1 u^{N-1} - a_2 u^{N-2} - \ldots - a_N;$$

then we have the following proposition.

D_m satisfies the linear recursion

$$D_{m+N} = a_1 D_{m+N-1} + a_2 D_{m+N-2} + \ldots + a_N D_m. \tag{38}$$

We can even go further and consider

$$F(u) = \prod_{i=1}^{R}(u - u_i) = u^R - b_1 u^{R-1} - b_2 u^{R-2} - \ldots - b_R :$$

from $F(u)$ we obtain for each of the classes A, B a "master recursion"

$$D_{m+R} = b_1 D_{m+R-1} + b_2 D_{m+R-2} + \ldots + b_R D_m \tag{39}$$

that is satisfied by all sequences $\{D_m\}$ where the tubules $T_n^* = T_{2m+1}^*$ are subject to the conditions described above, regardless of the particular shape of the holes (faces F_1, F_2) at the ends of the tubules T_1^* (note, however, that these holes determine the class – A or B – to which the T_n^* pertain).

If there is a dominant number u_{i_0} among the numbers $u_1, u_2, \ldots, u_N$ (i.e., such that u_{i_0} is positive and $|u_i| < u_{i_0}$ for $i \neq i_0$), then

$$\lim_{m\to\infty} \frac{K_{2m+3}}{K_{2m+1}} = \lim_{m\to\infty} \frac{D_{m+1}}{D_m} = \lim_{m\to\infty} |D_m|^{\frac{1}{m}} = u_{i_0}. \tag{40}$$

The number of faces of $T_n^* = T_{2m+1}^*$ being asymptotically equivalent to $(n-1)q = 2qm$, we conclude from (40) that

$$\begin{aligned} \lim_{m\to\infty} \kappa(T_{2m+1}^*) &= \lim_{m\to\infty} \frac{\log_2 |D_m|}{2qm} \\ &= \lim_{m\to\infty} \frac{m \log_2 |D_m|^{\frac{1}{m}}}{2qm} = \frac{1}{q} \log_2 \sqrt{u_{i_0}}. \end{aligned}$$

In any case,

$$|x_{js}| \leq \tfrac{1}{2}(3+\sqrt{5}) = \{\tfrac{1}{2}(1+\sqrt{5})\}^2,$$

thus

$$|u_i| \leq [\tfrac{1}{2}(1+\sqrt{5})]^{2p^*}, \quad i = 1, 2, \ldots, R$$

and

$$|D_m| = |\sum_{i=1}^{R} d_i u_i^m| \leq C'(\max_{i=1,2,\ldots,R} |u_i|)^m \leq C'\{\frac{1}{2}(1+\sqrt{5})\}^{2p^* m}$$

where C' is a constant.

We conclude that

$$\begin{aligned} \kappa(T_{2m+1}^*) &= \frac{\log_2 K_{2m+1}}{h(T_{2m+1}^*) + 1} \\ &< \frac{log_2 |D_m|}{2qm} \leq \frac{C}{m} + \frac{p^*}{q} \log_2 \{\tfrac{1}{2}(1+\sqrt{5})\} \end{aligned} \tag{41}$$

where C is a constant.

In particular, (41) implies

$$\limsup \kappa(T^*_{2m+1}) \leq \frac{p^*}{q} \log_2\{\frac{1}{2}(1+\sqrt{5})\} = \frac{p^*}{q} 0.6942419136\ldots. \tag{42}$$

(note the dependence of this limit on the number of peaks).

Let M_1, M_2 be the two perfect matchings of $\tilde{\mathcal{H}}_c$ whose edges are not perpendicular to the axis (see Section 4.3.1) and let $p^*_{ui}, v^*_{ui}; p^*_{li}, v^*_{li}$ be the numbers of peaks and of valleys of T^*_1 at the upper and at the lower end of T^*_1, respectively, induced by the acyclic matching $M_i|_{T^*_1}$ $(i = 1, 2)$. It can easily be proved that

$$p^*_{u1} - v^*_{u1} + p^*_{u2} - v^*_{u2} = v^*_{l1} - p^*_{l1} + v^*_{l2} - p^*_{l2} = 2q;$$

therefore, at least one of the two numbers

$$p^*_{u1} - v^*_{u1} = v^*_{l1} - p^*_{l1}, \quad p^*_{u2} - v^*_{u2} = v^*_{l2} - p^*_{l2}$$

does not exceed q. If, in particular,

$$v^*_{u1} = v^*_{u2} = p^*_{l1} = p^*_{l2} = 0 \tag{$*$}$$

(i.e., if there are no valleys at the upper end and no peaks at the lower end of T^*_1) then $p^*_{ui} = p^*_i = v^*_{li} = v^*_i$ $(i = 1, 2)$ and $\min(p^*_1, p^*_2) \leq q$. Now (42) implies

$$\begin{aligned} \limsup \kappa(T^*_{2m+1}) &\leq \log_2\{\tfrac{1}{2}(1+\sqrt{5})\} \\ &= 0.6942419136\ldots. \end{aligned} \tag{43}$$

In fact, (43) is true in any case – also if condition $(*)$ does not hold – but we will skip the proof.

4.3.6 The fully twisted normal tubule (Fig.19)

Let T_n denote the normal tubule occupying levels 0 through n. Its height is $(n-1)/2$, its circumference is twice the number p of peaks, i.e., $q = p$.

For the i-th components of the initial vectors

$$\mathbf{q}(P_k) = (\delta_{k1}, \delta_{k2}, \ldots, \delta_{kp})$$

(see Section 4.1), the initial values of the corresponding function $\varphi(k,n)$ (see equation (13′)) are

$$\begin{cases} \varphi(k,-1) &= 0 \\ \varphi(k,0) &= \delta_{ki}, \end{cases} \tag{44}$$

($k = 0, 1, \ldots, p-1$; subscript p is here replaced with subscript 0).

We will denote the special function $\varphi(k,n)$ determined by the initial values (44) by $\varphi^i(k,n)$. We start with $i = 0$ and calculate the corresponding coefficients A^s_{0j}, see end of Section 4.3.4. With $m_0 = -p$ and $\mu = r + p$ we obtain from (37) the equations

$$\sum_{j,s} z_{js}^{2r+1} A^s_{0j} = a_{0,r}, \quad -p \le r \le p-1.$$

The values $a_{0,r}$ are easily found using the scheme of Fig. 20 which immediately yields

$$a_{0,r} = \varphi(0, 2r) = 1, \quad -p \le r \le p-1,$$

see Fig. 21. Thus we have to solve the $2p$ linear equations

$$\sum_{j,s} z_{j,s}^{2r+1} A^s_{0j} = 1, \quad -p \le r \le p-1. \tag{45}$$

With $u_{js} = z_{js}^{-2p+1} A^s_{0j}$, (45) becomes

$$\begin{aligned} \sum_{j,s} z_{j,s}^{2\mu} u_{js} &= \sum_{j,s} x_{js}^{\mu} u_{js} = 1, \\ &\mu = 0, 1, \ldots, 2p-1. \end{aligned} \tag{46}$$

Let

$$x^*_{js} = \begin{cases} x_{js} & \text{if } (j,s) \neq (j^*, s^*) \\ 1 & \text{if } (j,s) = (j^*, s^*). \end{cases}$$

By Cramer's rule,

$$u_{j^*s^*} = \frac{D(j^*, s^*)}{D}$$

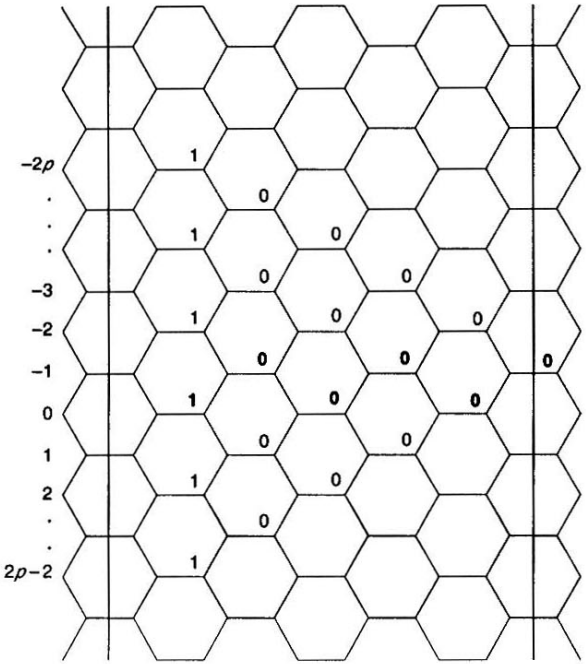

Figure 21.

where D and $D(j^*, s^*)$ are the Vandermonde determinants $V(x_{0+}, x_{0-}, \ldots, x_{p-1,+}, x_{p-1,-})$ and $V(x^*_{0+}, x^*_{0-}, \ldots, x^*_{p-1,+}, x^*_{p-1,-})$, respectively. Using "$<$" for the lexicographic order among the pairs (j, s), we obtain

$$D = \prod_{(j',s')<(j,s)} (x_{js} - x_{j's'}) \neq 0,$$
$$D(j^*, s^*) = \prod_{(j',s')<(j,s)} (x^*_{js} - x^*_{j's'}) \neq 0,$$

thus

$$u_{js} = \alpha\beta^{-1} \tag{47}$$

where

$$\alpha = \prod_{j',s':(j',s')\neq(j,s)} (x_{j's'} - 1),$$
$$\beta = \prod_{j',s':(j',s')\neq(j,s)} (x_{j's'} - x_{js}).$$

Using (19) we find

$$\begin{aligned}\prod_{j',s'} (x_{j's'} - 1) &= \prod_{j',s'} (1 - x_{j's'}) \\ &= \prod_{j',s'} (x - x_{j's'})|_{x=1} = (x-1)^{2p} - \delta x^p|_{x=1} \\ &= -\delta.\end{aligned}$$

Consequently, by (29),

$$\alpha = \frac{-\delta}{x_{js} - 1} = -\delta\eta_j^{-1} z_{js}^{-1}.$$

Similarly,

$$\begin{aligned}\beta &= -\prod_{j',s':(j',s')\neq(j,s)} (x_{js} - x_{j's'}) = -\lim_{x\to x_{js}} \frac{\prod_{j',s'} (x - x_{j's'})}{x - x_{js}} \\ &= -\frac{\mathrm{d}}{\mathrm{d}x}[(x-1)^{2p} - \delta x^p]_{x=x_{js}} = -p[2(x-1)^{2p-1} - \delta x^{p-1}]_{x=x_{js}} \\ &= -p\{2\frac{(x_{js}-1)^{2p}}{x_{js}-1} - \delta x_{js}^{p-1}\} = -p\{2\frac{\delta x_{js}^p}{x_{js}-1} - \delta x_{js}^{p-1}\}\end{aligned}$$

$$
\begin{aligned}
&= -\delta p x_{js}^{p-1}\{\frac{2x_{js}}{x_{js}-1}-1\} = -\delta p x_{js}^{p-1}\frac{x_{js}+1}{x_{js}-1} \\
&= -\delta p x_{js}^{p-1}\frac{4+\epsilon_j+sr_j}{\epsilon_j+sr_j}\times\frac{\epsilon_j-sr_j}{\epsilon_j-sr_j} = -\delta p x_{js}^{p-1}\frac{4\epsilon_j-4sr_j+\epsilon_j^2-\epsilon_j(4+\epsilon_j)}{\epsilon_j^2-\epsilon_j(4+\epsilon_j)} \\
&= -\delta p x_{js}^{p-1}\frac{-4sr_j}{-4\epsilon_j} = -s\delta x_{js}^{p-1}r_j\epsilon_j^{-1}p.
\end{aligned}
$$

Inserting the last two results into (47), we obtain

$$
\begin{aligned}
u_{js} &= \alpha\beta^{-1} = \eta_j^{-1}z_{js}^{-1}sx_{js}^{-p+1}r_j^{-1}\epsilon_j p^{-1} \\
&= sz_{js}^{-2p+1}\eta_j r_j^{-1}p^{-1}
\end{aligned}
$$

where we have used (27) and (28). Eventually, we have found

$$
A_{0j}^s = z_{js}^{2p-1}u_{js} = s\eta_j r_j^{-1}p^{-1}. \tag{48}
$$

Equations (36) now give us the explicit values of the coefficients A_{kj}^s, B_{kj}^s; using (27) we have

$$
\begin{cases}
A_{kj}^s = s\eta_j^{2k+1}r_j^{-1}p^{-1}, \\
B_{kj}^s = s\eta_j^{2k}r_j^{-1}p^{-1}.
\end{cases} \tag{49}
$$

By (14), (30) and (49),

$$
\begin{cases}
\varphi^0(k,2m+2) &= \sum_{j,s} A_{kj}^s z_{js}^{2m+3}, \\
\varphi^0(k,2m+1) &= \sum_{j,s} \eta_j^{-1}A_{kj}^s z_{js}^{2m+2}
\end{cases} \tag{50}
$$

where $A_{kj}^s = s\eta_j^{2k+1}r_j^{-1}p^{-1}$.

Let

$$
\begin{aligned}
R_j &= \begin{cases} \eta_j r_j^{-1}p^{-1}(z_{j+}^{n+2}-z_{j-}^{n+2}) & \text{if n is odd} \\ r_j^{-1}p^{-1}(z_{j+}^{n+2}-z_{j-}^{n+2}) & \text{if n is even,} \end{cases} \\
\alpha_k &= \varphi^0(k,n+1);
\end{aligned} \tag{51}
$$

(50) can then be briefly rewritten as

$$\alpha_k = \sum_{j=0}^{p-1} \epsilon_j^k R_j. \tag{50'}$$

Cases A and B need to be treated separately. Recall: we have case A if the orientation μ is Kasteleyn with respect to F_1 and case B if it is not. It is easy to check that a normal fully-twisted tubule T_n belongs to case A if the number p of its peaks is odd, and to case B otherwise.

Case A: $p \equiv 1, \mod 2$.

Let

$$S_n = \sum_{k=0}^{p-1} \varphi^0(k, n).$$

Clearly, S_n has initial values

$$S_{-1} = 0, \quad S_0 = 1$$

and, by (12') (where $\sigma_{k+1} = 1$), S_n satisfies the Fibonacci recursion

$$S_{n+2} = S_{n+1} + S_n$$

implying that S_n equals the Fibonacci number F_n. In particular, if $p = 1$ then

$$\varphi^0(0, n) = S_n = F_n.$$

Therefore, $\varphi^0(k, n)$ (p odd) may be considered a generalization of the Fibonacci sequence.

Note also that equation

$$y^{2p} = (y + 1)^p \tag{25A}$$

(which may be called the "intrinsic equation" of $\mathcal{H}_c$, case A) has precisely two real roots, namely

$$y_{0s} = \frac{1}{2}(1 + s\sqrt{5})$$

where $y_{0+} = \frac{1}{2}(1+\sqrt{5})$ is dominant. Further, $\eta_0 = \epsilon_0 = 1$, $r_0 = \sqrt{5}$; thus, by (49), in (50) the coefficients of the powers of the real roots $z_{0s} = y_{0s}$ are

$$A^s_{k0} = B^s_{k0} = \frac{s}{p\sqrt{5}}$$

(see also (35A) and the remark following it).

Since $\mathrm{sgn}(e) = 1$ for every edge of T_n, we have complete circular symmetry; thus it suffices to calculate only the first components $\varphi^0(k,n,-)$ of the vectors $\mathbf{q}(V_k)$, form the corresponding column vector (or row vector – it does not matter) and obtain from it the matrix $Q = (q_{ik})_{i,k=0,1,\ldots,p-1} = (\varphi^i(k,n,-))_{i,k=0,1,\ldots,p-1}$ (see Section 4.1) as a circulant matrix:

$$Q = Q_n = \mathrm{circ}(\varphi^0(0,n,-), \varphi^0(1,n,-), \ldots, \varphi^0(p-1,n,-)).$$

By (12), $\varphi^0(k,n,-)$ is equal to $\varphi^0(k,n+1)$ if n is even and to $\varphi^0(k-1,n+1)$ if n is odd: as we are only interested in $|\det Q|$, we may in both cases replace Q with the matrix

$$Q' = Q'_n = \mathrm{circ}(\varphi^0(0,n+1), \varphi^0(1,n+1), \ldots, \varphi^0(p-1,n+1))$$

whose entries $\varphi^0(k,n+1) = \alpha_k$ we know already (see (50)). Let

$$D_n = \det Q'_n.$$

By (11),

$$K(T_n) = |D_n|,$$

thus it remains to calculate

$$D_n = \det \mathrm{circ}(\alpha_0, \alpha_1, \ldots, \alpha_{p-1}).$$

Let

$$\zeta = e^{\frac{2\pi}{p}i};$$

then, by (26) and (27),

$$\epsilon_j = \eta_j^2 = \zeta^j$$

and (50′) becomes

$$\alpha_k = \sum_{j=0}^{p-1} \zeta^{jk} R_j. \tag{50′A}$$

Consider the polynomial

$$f_{Q'}(x) = \sum_{k=0}^{p-1} \alpha_k x^k. \tag{52}$$

As is well known (see [23], pp. 73-75), the eigenvalues λ_l and the determinant of Q' are

$$\lambda_l = f_{Q'}(\zeta^{-l}), \quad l = 0, 1, \ldots, p-1 \tag{53}$$

and

$$\det Q' = \prod_{l=0}^{p-1} \lambda_l = \prod_{l=0}^{p-1} f_{Q'}(\zeta^{-l}), \tag{54}$$

respectively. Using (50′A), (52) and (53), we obtain

$$\begin{aligned} \lambda_l &= \sum_{k=0}^{p-1} \sum_{j=0}^{p-1} \zeta^{jk} R_j \zeta^{-lk} = \sum_{j=0}^{p-1} \sum_{k=0}^{p-1} R_j \zeta^{(j-l)k} \\ &= \sum_{j=0}^{p-1} (\sum_{k=0}^{p-1} \zeta^{(j-l)k}) R_j = pR_l \end{aligned}$$

since

$$\sum_{k=0}^{p-1} \zeta^{(j-l)k} = \begin{cases} p & \text{if } j \equiv l, \bmod p \\ 0 & \text{otherwise.} \end{cases}$$

Thus, by (54) and (51),

$$D_n = \det Q' = \prod_{l=0}^{p-1} (pR_l) = ABC$$

where

$$\begin{aligned} A &= \begin{cases} \prod_{j=0}^{p-1} \eta_j & \text{if } n \text{ is odd} \\ 1 & \text{if } n \text{ is even,} \end{cases} \\ B &= (\prod_{j=0}^{p-1} r_j)^{-1}, \\ C &= \prod_{j=0}^{p-1} (z_{j+}^{n+2} - z_{j-}^{n+2}). \end{aligned}$$

We have

$$A = \begin{cases} \prod_{j=0}^{p-1} e^{\frac{j}{p}\pi i} = e^{\frac{p-1}{2}\pi i} = (-1)^{\frac{p-1}{2}} & \text{if n is odd} \\ 1 & \text{if n is even,} \end{cases}$$

thus $|A| = 1$;

$$\begin{aligned} B^{-2} &= \prod_{j=0}^{p-1} \{\epsilon_j (4 + \epsilon_j)\} = \prod_{j=0}^{p-1} \epsilon^{2j} \prod_{l=0}^{p-1} (4 + \epsilon^{2l}) \\ &= -\prod_{l=0}^{p-1} (-4 - \epsilon^{2l}) = -(x^p - 1)|_{x=-4} \\ &= 4^p + 1 \end{aligned} \tag{55}$$

(note that $\epsilon^2 = e^{\frac{2\pi}{p}i}$ is a primitive p-th root of unity);

$$\begin{aligned} C &= \prod_{j=0}^{p-1} [(\eta_j^{-1} y_{j+})^{n+2} - (\eta_j^{-1} y_{j-})^{n+2}] \\ &= (\prod_{l=0}^{p-1} \eta_l)^{-n-2} \prod_{j=0}^{p-1} (y_{j+}^{n+2} - y_{j-}^{n+2}) \\ &= (-1)^{\frac{p-1}{2}(n+2)} \prod_{j=0}^{p-1} (y_{j+}^{n+2} - y_{j-}^{n+2}). \end{aligned}$$

Consequently,

$$\begin{aligned} K(T_n) &= |D_n| = |ABC| \\ &= (4^p + 1)^{-\frac{1}{2}} |\prod_{j=0}^{p-1} (y_{j+}^{n+2} - y_{j-}^{n+2})|. \end{aligned} \tag{56}$$

With $p = 1$ we return to the Fibonacci numbers.

Case B: $p \equiv 0$, mod 2.

Having determined the coefficients of $\varphi^0(k,n)$ for both cases A and B (equation (50)), we will now calculate the coefficients of $\varphi^i(k,n)$, $i = 1, 2, \ldots, p-1$, for case B.

Let us recall the definition of the function $\varphi^i(k,n)$ for case B from (12′) and (44):

$$\begin{cases} \varphi^i(k,2m+3) = \varphi^i(k,2m+2) + \varphi^i(k,2m+1) \\ \varphi^i(k,2m+2) = \sigma_{k+1}\varphi^i(k+1,2m+1) + \varphi^i(k,2m) \\ \text{where } \sigma_k = \begin{cases} -1 \text{ if } k \equiv 0, \text{ mod } p \\ 1 \text{ otherwise;} \end{cases} \\ \varphi^i(k,-1) = 0,\ \varphi^i(k,0) = \delta_{ki}\ (i, k \bmod p). \end{cases} \tag{57}$$

Define

$$\vartheta_k^i = \begin{cases} 1 & \text{for } k = 0,1,\ldots,p-1-i \\ -1 & \text{for } k = p-i, p-i+1, \ldots, p-1 \\ & (i,k = 0,1,\ldots,p-1) \end{cases} \tag{58}$$

(Fig. 22).

Note that $\vartheta_0^i = 1$ for all values of i.

Lemma 4.1

$$\sigma_{k+i+1}\vartheta_k^i\vartheta_{k+1}^i = \sigma_{k+1}. \tag{59}$$

Proof. We have

$$\vartheta_k^i\vartheta_{k+1}^i = \begin{cases} -1 & \text{if } k = p-1 \text{ or } k = p-1-i \\ 1 & \text{otherwise} \end{cases}$$

(Fig. 22),

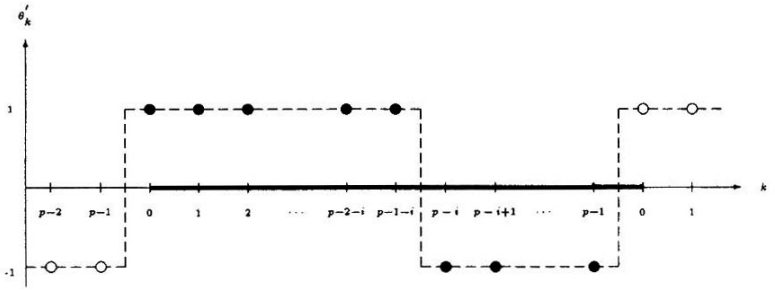

Figure 22.

$$\sigma_{k+i+1} = \begin{cases} -1 & \text{if } k = p-1-i \\ 1 & \text{otherwise,} \end{cases}$$

thus

$$\sigma_{k+i+1}\vartheta_k^i\vartheta_{k+1}^i = \left\{ \begin{array}{ll} -1 & \text{if } k = p-1 \\ 1 & \text{otherwise} \end{array} \right\} = \sigma_{k+1}.$$

□

Claim.

$$\varphi^i(k+i,n) = \vartheta_k^i\varphi^0(k,n). \tag{60}$$

Proof. By induction on n. The claim is true for $n = -1, 0$. Suppose it is true for $n = 2m+1$. $2m+2$ $(m \geq -1)$. We shall show that it is also true for $n = 2m+3$, $2m+4$.

Using (57) and the induction hypothesis, we obtain

$$\begin{aligned} \varphi^i(k+i,2m+3) &= \varphi^i(k+i,2m+2) + \varphi^i(k+i,2m+1) \\ &= \vartheta_k^i\varphi^0(k,2m+2) + \vartheta_k^i\varphi^0(k,2m+1) \\ &= \vartheta_k^i\varphi^0(k,2m+3); \end{aligned}$$

in the same way, using the last result and Lemma 4.1:

$$\varphi^i(k+i,2m+4) = \sigma_{k+i+1}\varphi^i(k+i+1,2m+3) + \varphi^i(k+i,2m+2)$$

$$
\begin{aligned}
&= \sigma_{k+i+1}\vartheta^i_{k+1}\varphi^0(k+1,2m+3) + \vartheta^i_k\varphi^0(k,2m+2)\\
&= \vartheta^i_k\{\sigma_{k+i+1}\vartheta^i_{k+1}\vartheta^i_k\varphi^0(k+1,2m+3) + \varphi^0(k,2m+2)\}\\
&= \vartheta^i_k\{\sigma_{k+1}\varphi^0(k+1,2m+3) + \varphi^0(k,2m+2)\}\\
&= \vartheta^i_k\varphi^0(k,2m+4).
\end{aligned}
$$

Both results taken together:

$$\varphi^i(k+i,n) = \vartheta^i_k\varphi^0(k,n)$$

for $n = 2m+3,\ 2m+4$.

This proves that (60) holds for $n \geq -1$; in an analogous way it can be shown that (60) is valid for $n < -1$, thus for all values of n. □

This means that – except for the sign which is determined by ϑ^i_k – the values $\varphi^i(k,n)$ can be expressed through the values $\varphi^0(k,n)$ for even p in the same way as for odd p.

Recall: $K(T_n) = |D_n|$ where $D_n = \det Q'$,

$$Q' = Q'_n = (\varphi^i(k,n+1))_{i,k=0,1,\ldots,p-1}.$$

By (60),

$$\varphi^i(k,n+1) = \varphi^i(k-i+i,n+1) = \vartheta^i_{k-i}\varphi^0(k-i,n+1)$$

where

$$\vartheta^i_{k-i} = \begin{cases} -1 & \text{for } k = 0,1,\ldots,i-1 \\ 1 & \text{for } k = i,i+1,\ldots,p-1. \end{cases}$$

Let $S = (\vartheta^i_{k-i})_{i,k=0,1,\ldots,p-1}$; clearly

$$S = \begin{pmatrix} 1 & 1 & 1 & .. & 1 & 1 & 1 \\ -1 & 1 & 1 & .. & 1 & 1 & 1 \\ -1 & -1 & 1 & .. & 1 & 1 & 1 \\ \vdots & \vdots & \vdots & :: & \vdots & \vdots & \vdots \\ -1 & -1 & -1 & .. & 1 & 1 & 1 \\ -1 & -1 & -1 & .. & -1 & 1 & 1 \\ -1 & -1 & -1 & .. & -1 & -1 & 1 \end{pmatrix}_{p\times p}$$

and $Q' = (\vartheta^i_{k-i}\varphi^0(k-i,n+1))$ is obtained from S and

$$(\varphi^0(k-i,n+1)) = \mathrm{circ}(\varphi^0(0,n+1),\varphi^0(1,n+1),\ldots,\varphi^0(p-1,n+1))$$

by elementwise multiplication; that means that Q' is a skew-circulant matrix, namely,

$$Q' = \operatorname{scirc}(\alpha_0, \alpha_1, \ldots, \alpha_{p-1})$$

where $\alpha_k = \varphi^0(k, n+1)$ (see [23], p. 83).

det Q' can now be found in a similar way as in case A. The eigenvalues of Q' are

$$\lambda_l = f_{Q'}(\epsilon^{-2l-1}), \quad l = 0, 1, \ldots, p-1 \tag{61}$$

where

$$f_{Q'}(x) = \sum_{k=0}^{p-1} \alpha_k x^k, \quad \epsilon = e^{\frac{\pi}{p} i}$$

(see [23], p. 84, nos. 4 and 6).

By (26) and (27), (50′) becomes

$$\alpha_k = \sum_{j=0}^{p-1} \epsilon^{(2j+1)k} R_j \tag{50'B}$$

and (61) yields, as in case A,

$$\lambda_l = \sum_{k=0}^{p-1} \sum_{j=0}^{p-1} \epsilon^{(2j+1)k} R_j \epsilon^{(-2l-1)k} = \sum_{j=0}^{p-1} \sum_{k=0}^{p-1} \epsilon^{2(j-l)k} R_j = p R_l.$$

Thus

$$\begin{aligned} D_n &= \det Q' = \prod_{l=0}^{p-1} (p R_l) \\ &= ABC \end{aligned}$$

where A, B, C are the same expressions as in case A. We obtain

$$A = \begin{cases} \prod_{j=0}^{p-1} \eta_j = \prod_{j=0}^{p-1} e^{\frac{2j+1}{2p}\pi i} = e^{\frac{p^2}{2p}\pi i} = (-1)^{\frac{p}{2}} & \text{if } n \text{ is odd,} \\ 1 \qquad \text{if } n \text{ is even,} \end{cases}$$

thus

$$|A| = 1;$$

$$\begin{aligned} B^{-2} &= \prod_{j=0}^{p-1}\{\epsilon_j(4+\epsilon_j)\} = \prod_{j=0}^{p-1}\epsilon^{2j+1}\prod_{l=0}^{p-1}(4+\epsilon^{2j+1}) \\ &= \prod_{j=0}^{p-1}(-4-\epsilon^{2j+1}) = (x^p+1)|_{x=-4} = 4^p+1; \end{aligned} \tag{62}$$

$$\begin{aligned} C &= \prod_{j=0}^{p-1}[(\eta_j^{-1}y_{j+})^{n+2} - (\eta_j^{-1}y_{j-})^{n+2}] = (\prod_{l=0}^{p-1}\eta_l)^{-n-2}\prod_{j=0}^{p-1}(y_{j+}^{n+2} - y_{j-}^{n+2}) \\ &= (-1)^{\frac{p}{2}(n+2)}\prod_{j=0}^{p-1}(y_{j+}^{n+2} - y_{j-}^{n+2}). \end{aligned}$$

Thus we have obtained the same formula as in case A (formula (56)), i.e., we have

Theorem 4.1

$$K(T_n) = \frac{1}{\sqrt{4^p+1}}|\prod_{j=0}^{p-1}(y_{j+}^{n+2} - y_{j-}^{n+2})| \tag{63}$$

where

$$y_{js} = \frac{1}{2}\{\epsilon_j + s\sqrt{\epsilon_j(4+\epsilon_j)}\} \quad (j = 0,1,\ldots,p-1, s = +1,-1),$$

$$\epsilon_j = \begin{cases} e^{\frac{j}{p}2\pi i} & \text{if } p \text{ is odd,} \\ e^{\frac{2j+1}{p}\pi i} & \text{if } p \text{ is even.} \end{cases}$$

□

In calculating B (formulae (55), (62)) we found

$$\prod_{j=0}^{p-1}\{\epsilon_j(4+\epsilon_j)\} = \prod_{j=0}^{p-1} r_j^2 = 4^p+1,$$

valid for all values of p. Note that $y_{j+} - y_{j-} = r_j$, thus

$$|\prod_{j=0}^{p-1}(y_{j+}-y_{j-})| = \sqrt{4^p+1}. \tag{64}$$

Combined with (63), this gives another explicit formula for $K(T_n)$, namely:

Corollary 4.1

$$K(T_n) = |\prod_{j=0}^{p-1} U_n^{(j)}| \tag{65}$$

where

$$U_n^{(j)} = \frac{y_{j+}^{n+2} - y_{j-}^{n+2}}{y_{j+} - y_{j-}}.$$

□

By their definition, y_{j+} and y_{j-} satisfy $y^2 = \epsilon_j(y+1)$; therefore, for fixed j the numbers $U_n^{(j)}$ satisfy the "quasi Fibonacci" recurrence relation

$$U_{n+2}^{(j)} = \epsilon_j(U_{n+1}^{(j)} + U_n^{(j)}) \tag{66}$$

with initial values

$$U_{-2}^{(j)} = 0, \quad U_{-1}^{(j)} = 1$$

from which they can easily be calculated. So we have found the following simple recursion procedure for obtaining $K(T_n)$.

Corollary 4.2 *To calculate $K(T_n)$, first calculate the "quasi Fibonacci" numbers $U_n^{(j)}$ for $j = 0, 1, \ldots, p-1$* (equations (66))*: the module of the product of these p numbers is equal to $K(T_n)$.* □

Note that

$$\begin{cases} \epsilon_{p-j} &= e^{\frac{p-j}{p}2\pi i} = e^{-\frac{j}{p}2\pi i} = \bar{\epsilon_j} & \text{if } p \text{ is odd} \\ \epsilon_{p-j-1} &= e^{\frac{2(p-j)-1}{p}\pi i} = e^{-\frac{2j+1}{p}\pi i} = \bar{\epsilon_j} & \text{if } p \text{ is even} \end{cases} \tag{67}$$

implying

$$\begin{cases} U_n^{(p-j)} = \bar{U}_n^{(j)} & \text{if } p \text{ is odd} \\ U_n^{(p-j-1)} = \bar{U}_n^{(j)} & \text{if } p \text{ is even.} \end{cases} \tag{68}$$

Inserting (68) into (65), we obtain

Corollary 4.3

$$K(T_n) = \begin{cases} F_{n+1} |\prod_{j=1}^{\frac{p-1}{2}} U_n^{(j)}|^2 & \textit{if } p \textit{ is odd} \\ |\prod_{j=0}^{\frac{p}{2}-1} U_n^{(j)}|^2 & \textit{if } p \textit{ is even} \end{cases} \tag{69}$$

where $F_n = U_{n-1}^{(0)}$ is the n-th Fibonacci number ($F_0 = F_1 = 1,\ F_2 = 2$). □

Let

$$\mathbf{S} = \{(s_0, s_1, \ldots, s_{p-1}) |\ s_j \in \{+1, -1\},\ j = 0, 1, \ldots, p-1\};$$

for $\mathbf{s} = (s_0, s_1, \ldots, s_{p-1}) \in \mathbf{S}$ define

$$w_{\mathbf{s}} = w_{s_0, s_1, \ldots, s_{p-1}} = \prod_{j=0}^{p-1} y_{j s_j}, \qquad \sigma(\mathbf{s}) = \prod_{j=0}^{p-1} s_j;$$

clearly, $\sigma(\mathbf{s}) = (-1)^{\nu(\mathbf{s})}$ where $\nu(\mathbf{s})$ is the number of negative components (minus signs) of $\mathbf{s}$.

From (63) we immediately obtain

Corollary 4.4

$$K(T_n) = |W_n| \quad \textit{where} \quad W_n = \frac{1}{\sqrt{4^p + 1}} \sum_{\mathbf{s} \in \mathbf{S}} \sigma(\mathbf{s}) w_{\mathbf{s}}^{n+2}.$$

□

For practical calculations Corollary 4.4 is of restricted value since the number of terms is 2^p. However, it shows that W_n satisfies a linear recursion relation and it enables the asymptotic behavior of $K(T_n)$ to be determined.

The recurrence relation for W_n

Let

$$F(w) = \prod_{\mathbf{s}\in\mathbf{S}} (w - w_{\mathbf{s}}) = w^r - A_1 w^{r-1} - A_2 w^{r-2} - \cdots - A_r$$

where $r = 2^p$.

Clearly, W_n satisfies

$$W_{n+r} = A_1 W_{n+r-1} + A_2 W_{n+r-2} + \cdots + A_r W_n. \tag{70}$$

$F(w)$ can be calculated algebraically from the roots y_{j_s} of $y^{2^p} = \delta(y+1)^p$ (equation (25)) or, in an elementary way, by successive elimination of the sign variables $s_0, s_1, \ldots, s_{p-1}$ from the expression

$$w = \prod_{j=0}^{p-1} \{\frac{1}{2}(\epsilon_j + s_j\sqrt{\epsilon_j(4+\epsilon_j)})\}$$

which requires p squaring operations.

The asymptotic behavior of $K(T_n)$

Let $\mathbf{s}_0 = (1, 1, \ldots, 1)$, and $w_0 = w_{\mathbf{s}_0} = w_{+++\ldots+}$.

First we shall show that the set $\{w_{\mathbf{s}} | \mathbf{s} \in \mathbf{S}\}$ is dominated by w_0, i.e., we shall show that

(a) w_0 is positive,

(b) $w_0 > |w_{\mathbf{s}}|$ for all $\mathbf{s} \in \mathbf{S} - \{\mathbf{s}_0\}$.

Note that each of the 2^p numbers $w_{\mathbf{s}} = \prod_{j=0}^{p-1} y_{j_{s_j}}$ picks up as a factor exactly one of the two roots of each of the equations

$$y^2 = \epsilon_j(y+1), \quad j = 0, 1, \ldots, p-1. \tag{23}$$

Let

$$j^* = \begin{cases} p-j & \text{if } p \text{ is odd} \\ p-j-1 & \text{if } p \text{ is even.} \end{cases}$$

By (67), the numbers ϵ_j and ϵ_{j^*} are complex conjugates, and so are the numbers r_j, r_{j^*} and the roots y_{js}, y_{j^*s} :

$$y_{j^*s} = \bar{y}_{js}. \tag{71}$$

For an auxiliary consideration, define

$$\begin{aligned} r(\varphi) &= \sqrt{e^{i\varphi}(4+e^{i\varphi})}, \\ f_s(\varphi) &= \tfrac{1}{2}\{e^{i\varphi} + sr(\varphi)\}, \quad s \in \{+1, -1\}. \end{aligned}$$

Note that

$$|f_s(\varphi)||f_{-s}(\varphi)| = 1, \tag{72}$$

$$r(\varphi)r(-\varphi) = |r(\varphi)|^2 = \sqrt{17 + 8cos\varphi} \tag{73}$$

and

$$y_{js} = f_s(\varphi_j) \tag{74}$$

where

$$\varphi_j = \begin{cases} \frac{2j}{p}\pi & \text{if } p \text{ is odd} \\ \frac{2j+1}{p}\pi & \text{if } p \text{ is even.} \end{cases}$$

Next we calculate $|f_s(\varphi)|^2$ for $0 \le \varphi < \pi$. We have

$$\begin{aligned} |f_s(\varphi)|^2 &= f_s(\varphi)f_s(-\varphi) = \frac{1}{4}\{e^{i\varphi} + sr(\varphi)\}\{e^{-i\varphi} + sr(-\varphi)\} \qquad (75) \\ &= \frac{1}{4}\{1 + r(\varphi)r(-\varphi) + 2s\varrho(\varphi)\} \quad \text{where } \varrho(\varphi) = Re(e^{i\varphi}r(-\varphi)). \end{aligned}$$

An elementary discussion shows that

$$\varrho(\varphi) > 0 \quad \text{for } 0 \le \varphi < \pi, \tag{76}$$

thus

$$\begin{aligned} e^{i\varphi}r(-\varphi) &= e^{i\varphi}\sqrt{e^{-i\varphi}(4+e^{-i\varphi})} \\ &= \sqrt{1+4e^{i\varphi}} = \sqrt{1+4cos\varphi+i\cdot 4sin\varphi}; \end{aligned}$$

by (22),

$$\varrho(\varphi) = \tfrac{1}{\sqrt{2}}\sqrt{\sqrt{17+8cos\varphi}+1+4cos\varphi} > 0, \quad 0 \le \varphi < \pi. \tag{77}$$

Inserting (73) and (77) into (75), we obtain

$$|f_s(\varphi)|^2 = \tfrac{1}{4}\{1+\sqrt{17+8cos\varphi}+s\sqrt{2}\sqrt{\sqrt{17+8cos\varphi}+1+4cos\varphi}\}, \quad 0 \le \varphi < \pi. \tag{78}$$

We conclude that

$$|f_+(\varphi)| > |f_-(\varphi)|,$$

and, by virtue of (72),

$$|f_+(\varphi)| > 1 > |f_-(\varphi)|, \quad 0 \le \varphi < \pi. \tag{79}$$

For $0 \le j \le \lfloor \frac{p-1}{2} \rfloor$, (79) implies

$$|y_{j+}| = |f_+(\varphi_j)| > 1 > |f_-(\varphi_j)| = |y_{j-}|;$$

for $\lfloor \frac{p-1}{2} \rfloor < j \le p-1$ we have $0 \le j^* \le \lfloor \frac{p-1}{2} \rfloor$ and again,

$$\begin{aligned} |y_{j+}| &= |y_{j^*+}| = |f_+(\varphi_{j^*})| > 1 \\ &> |f_-(\varphi_{j^*})| = |y_{j^*-}| = |y_{j-}|. \end{aligned}$$

Thus we have found

$$|y_{j+}| > 1 > |y_{j-}|, \quad j = 0, 1, \ldots, p-1. \tag{80}$$

By (71),

$$w_0 = w_{\mathbf{s}_0} = \prod_{j=0}^{p-1} y_{j+} = \begin{cases} \frac{1}{2}(1+\sqrt{5}) \prod_{j=1}^{\frac{p-1}{2}} |y_{j+}|^2 & \text{if } p \text{ is odd} \\ \prod_{j=0}^{\frac{p}{2}-1} |y_{j+}|^2 & \text{if } p \text{ is even.} \end{cases} \tag{81}$$

Inequality (80) now immediately implies

$$w_0 > 1, \tag{82}$$

$$w_0 > \prod_{j=0}^{p-1} |y_{j s_j}| = |w_{\mathbf{s}}| \tag{83}$$

for every $\mathbf{s} = (s_0, s_1, \ldots, s_{p-1}) \in S - \{\mathbf{s}_0\}$.

This means that w_0 indeed dominates the set $\{w_{\mathbf{s}} |\ \mathbf{s} \in S\}$. Combining this result with Corollary 4.4, we see that, for sufficiently large values of n,

$$K(T_n) = W_n = \frac{1}{\sqrt{4^p+1}} \sum_{\mathbf{s} \in \mathbf{S}} \sigma(\mathbf{s}) w_{\mathbf{s}}^{n+2} \tag{84}$$

implying

$$\frac{K(T_n)}{w_0^{n+2}} = \frac{1}{\sqrt{4^p+1}} \{1 + \sum_{\mathbf{s} \in \mathbf{S} - \{\mathbf{s}_0\}} \sigma(\mathbf{s}) (\frac{w_{\mathbf{s}}}{w_0})^{n+2}\}$$

where the last sum tends to zero when n tends to infinity. Thus we obtain the following proposition.

Theorem 4.2

$$\lim_{n \to \infty} \frac{K(T_n)}{w_0^{n+2}} = \frac{1}{\sqrt{4^p+1}}, \tag{85}$$

$$\lim_{n \to \infty} \frac{K(T_{n+1})}{K(T_n)} = w_0, \tag{86}$$

$$\lim_{n \to \infty} K(T_n)^{\frac{1}{n}} = w_0. \tag{87}$$

□

By (87)

$$\lim_{n \to \infty} \frac{1}{n} \log_2 K(T_n) = \log_2 w_0;$$

using the fact that T_n has $f_n = (n-1)p + 2$ faces, we obtain

Corollary 4.5

$$\lim_{n\to\infty} \kappa(T_n) = \lim_{n\to\infty} \frac{\log_2 K(T_n)}{f_n - 1} = \frac{1}{p} \log_2 w_0. \tag{88}$$

□

(Note that, because of (82), $\log_2 w_0 > 0$.) As w_0 and $\lim_{n\to\infty} \kappa(T_n)$ depend on p (and only on p), we will write

$$w_0 = w(p), \quad \frac{1}{p} \log_2 w_0 = \kappa(p).$$

$w(p)$ and $\kappa(p)$ can easily be calculated: using (74),(78),(81) and (88), we obtain

Theorem 4.3

$$\begin{aligned} w(p) = \; & \tfrac{1}{2^p}(1+\sqrt{5}) \prod_{j=1}^{\frac{p-1}{2}} \{1 + \sqrt{17 + 8cos\tfrac{2j}{p}\pi} \\ & + \sqrt{2}\sqrt{\sqrt{17 + 8cos\tfrac{2j}{p}\pi} + 1 + 4cos\tfrac{2j}{p}\pi}\} \quad \textit{if } p \textit{ is odd,} \end{aligned} \tag{89A}$$

$$\begin{aligned} w(p) = \; & \tfrac{1}{2^p} \prod_{j=0}^{\frac{p}{2}-1} \{1 + \sqrt{17 + 8cos\tfrac{2j+1}{p}\pi} \\ & + \sqrt{2}\sqrt{\sqrt{17 + 8cos\tfrac{2j+1}{p}\pi} + 1 + 4cos\tfrac{2j+1}{p}\pi}\} \quad \textit{if } p \textit{ is even;} \end{aligned} \tag{89B}$$

$$\begin{aligned} \kappa(p) \; = \; & \tfrac{1}{p}\{-p + \log_2(1+\sqrt{5}) \\ & + \sum_{j=1}^{\frac{p-1}{2}} \log_2[1 + \sqrt{17 + 8cos\tfrac{2j}{p}\pi} \\ & + \sqrt{2}\sqrt{\sqrt{17 + 8cos\tfrac{2j}{p}\pi} + 1 + 4cos\tfrac{2j}{p}\pi}]\} \quad \textit{if } p \textit{ is odd,} \end{aligned} \tag{90A}$$

$$\begin{aligned} \kappa(p) \; = \; & \tfrac{1}{p}\{-p + \sum_{j=0}^{\frac{p}{2}-1} \log_2[1 + \sqrt{17 + 8cos\tfrac{2j+1}{p}\pi} \\ & + \sqrt{2}\sqrt{\sqrt{17 + 8cos\tfrac{2j+1}{p}\pi} + 1 + 4cos\tfrac{2j+1}{p}\pi}]\} \; \textit{if } p \textit{ is even.} \end{aligned} \tag{90B}$$

□

Writing (90B) in the form

$$\kappa(p) = -1 + \frac{1}{2} \times \frac{1}{p/2} \sum_{j=0}^{\frac{p}{2}-1} \log_2[\cdots]$$

and letting p tend to infinity, we immediately obtain

$$\begin{aligned} \lim_{p\to\infty, p\ even} \kappa(p) &= \frac{1}{2\pi}\int_0^{\pi} \log_2[1+\sqrt{17+8cos\varphi} \\ &\quad +\sqrt{2}\sqrt{\sqrt{17+8cos\varphi}+1+4cos\varphi}]d\varphi - 1 \\ &= 0.4660856399\ldots. \end{aligned}$$

In the same way, we obtain the analogous result also from (90A):

$$\lim_{p\to\infty,\, p\ odd} \kappa(p) = 0.4660856399\ldots.$$

Thus we have

Corollary 4.6

$$\begin{aligned} \lim_{p\to\infty} \kappa(p) &= \frac{1}{2\pi}\int_0^{\pi} \log_2[1+\sqrt{17+8cos\varphi} \\ &\quad +\sqrt{2}\sqrt{\sqrt{17+8cos\varphi}+1+4cos\varphi}]d\varphi - 1 \\ &= 0.4660856399\ldots. \end{aligned}$$

□

The simplest cases $p = 2$ and $p = 3$.

$\underline{p = 2.}$

Intrinsic equation:

$$y^4 + (y+1)^2 = 0.$$

Intrinsic roots:

$$\begin{aligned} y_{0s} &= \frac{1}{2}(i + s\sqrt{-1+4i}) \\ &= \frac{s}{2\sqrt{2}}\sqrt{\sqrt{17}-1} + i(1+\frac{s}{2\sqrt{2}}\sqrt{\sqrt{17}+1}), \\ y_{1s} &= \bar{y}_{0s} \quad (s \in \{+1,-1\}). \end{aligned}$$

Root products:

$$\begin{aligned} w_{s_0 s_1} &= y_{0 s_0} y_{1 s_1} \\ &= \frac{1}{4}[1 + s_0 s_1 \sqrt{17} + (s_1 + s_0)\frac{1}{\sqrt{2}}\sqrt{\sqrt{17}+1}] \\ &\quad + i(s_1 - s_0)\frac{1}{4\sqrt{2}}\sqrt{\sqrt{17}-1}. \end{aligned}$$

Asymptotic growth factor:

$$\begin{aligned} w(2) &= w_{++} = \frac{1}{4}(1 + \sqrt{17} + \sqrt{2}\sqrt{\sqrt{17}+1}) \\ &= 2.081018997\ldots. \end{aligned}$$

Limit of Kekulé index:

$$\kappa(2) = \frac{1}{2}\log_2 w_0 = 0.528645067\ldots.$$

In this case, $W_n > 0$, thus $K(T_n) = W_n$.

Recurrence formula for $K_n = K(T_n)$:

$$K_{n+4} = K_{n+3} + 2K_{n+2} + K_{n+1} - K_n.$$

Initial values:

$$K_{-3} = 1,\ K_{-2} = 0,\ K_{-1} = 1,\ K_0 = 1.$$

$\underline{p = 3.}$

Intrinsic equation:

$$y^6 - (y+1)^3 = 0.$$

Intrinsic roots:

$$y_{0s} = \frac{1}{2}(1 + s\sqrt{5}),$$

$$\begin{aligned} y_{1s} &= \frac{1}{2}(-\frac{1}{2}+i\frac{\sqrt{3}}{2}+s\sqrt{-\frac{5}{2}+i\frac{3\sqrt{3}}{2}}) \\ &= \frac{1}{4}\{-1+s\sqrt{2}\sqrt{\sqrt{13}-\frac{5}{2}}+i(\sqrt{3}+s\sqrt{2}\sqrt{\sqrt{13}+\frac{5}{2}})\}, \\ y_{2s} &= \bar{y}_{1s} \quad (s\in\{+1,-1\}). \end{aligned}$$

Root products:

$$\begin{aligned} w_{s_0s_1s_2} &= y_{0s_0}y_{1s_1}y_{2s_2} \\ &= \frac{1}{8}\{1+s_0\sqrt{5}+s_1s_2\sqrt{13}+s_0s_1s_2\sqrt{65} \\ &\quad +(1+s_0\sqrt{5})(s_1+s_2)\frac{1}{\sqrt{2}}\sqrt{\sqrt{13}-1} \\ &\quad +i(1+s_0\sqrt{5})(s_2-s_1)\frac{1}{\sqrt{2}}\sqrt{\sqrt{13}+1}\}. \end{aligned}$$

Asymptotic growth factor:

$$\begin{aligned} w(3) &= w_{+++} = \frac{1}{8}\{1+\sqrt{5}+\sqrt{13}+\sqrt{65}+\sqrt{2}(1+\sqrt{5})\sqrt{\sqrt{13}-1}\} \\ &= 2.786390129\ldots. \end{aligned}$$

Limit of Kekulé index:

$$\kappa(3) = \frac{1}{3}\log_2 w_0 = 0.492799089\ldots.$$

Again, $W_n > 0$, thus $K(T_n) = W_n$.

Recurrence formula for $K_n = K(T_n)$:

$$K_{n+8} = K_{n+7} + 4K_{n+6} + 5K_{n+5} - 5K_{n+4} - 5K_{n+3} + 4K_{n+2} - K_{n+1} - K_n.$$

Initial values:

$$K_{-5} = 2,\ K_{-4} = -1,\ K_{-3} = 1,\ K_{-2} = 0, K_{-1} = 1,\ K_0 = 1,\ K_1 = 2,\ K_2 = 9.$$

*

Some numerical results are contained in the Appendix.

5 Concluding remark

The above investigations have led to the result that the Kekulé index of (not-too-small) untwisted normal tubules is small and tends to zero with increasing circumference (Section 4.2) whereas the Kekulé index of fully twisted normal tubules lies above 0.466 (see Figs. 23a, 23b in the Appendix). The investigations can be extended to cylindrical hexagonal tessellations and tubules of any possible twist: each of these tessellations has a pair of intrinsic equations (one for case A and one for case B) which are similar to those we have discussed above but of an algebraically more complex nature. A first discussion of these equations and their roots seems to indicate the general tendency that the Kekulé index increases with increasing twist – a statement which can here be made only tentatively; more precise propositions require deeper investigations.

We have considered tubules with "open ends" only. Tubules which represent fullerenes – i.e., pure carbon molecules of tubular shape which have a cap at each end consisting of hexagons and precisely 6 pentagons each – may behave differently. For the special fullerene tubule $T^*(n,5)$ which consists of an untwisted tubule $T(n,5)$ (see Fig. 17) capped at its ends by the two halves of a pentagon-dodecahedron we found the formula

$$K_n^* = K(T^*(n,5)) = 5^{n+2} + (\sqrt{5})^{n+2}\{(\frac{\sqrt{5}+1}{2})^n + (\frac{\sqrt{5}-1}{2})^n\} + 1;$$

the K_n^* satisfy the (linear but non-homogeneous) recurrence relation

$$K_{n+3}^* = 10K_{n+2}^* - 30K_{n+1}^* + 25K_n^* - 4$$

with initial values

$$K_0^* = 36, \quad K_1^* = 151, \quad K_2^* = 701.$$

However, it should be mentioned that for fullerenes – i.e., if pentagons are present – the significance of the Kekulé count for the stability of the molecule is not well known and needs further investigation; maybe, the edges (bonds) should be weighted according to the number of pentagons (none, one or two) to which they belong.

6 Appendix

Some numerical results for fully twisted tubules of circumference $2p$, $p = 2, 3, \ldots, 13$. $q = q_n = K(T_n)/K(T_{n-1})$.

# of columns of hexagons=4			
n-1	K	q	κ
1	5.000000×10^{0}	2.500000	0.773976
2	9.000000×10^{0}	1.800000	0.633985
3	2.000000×10^{1}	2.222222	0.617418
4	4.100000×10^{1}	2.050000	0.595284
5	8.500000×10^{1}	2.073171	0.582672
6	1.780000×10^{2}	2.094118	0.575056
7	3.690000×10^{2}	2.073034	0.568498
8	7.690000×10^{2}	2.084011	0.563932
9	1.600000×10^{3}	2.080624	0.560203
10	3.329000×10^{3}	2.080625	0.557184
15	1.299400×10^{5}	2.081004	0.547983
20	5.071361×10^{6}	2.081019	0.543267
25	1.979269×10^{8}	2.081019	0.540400
30	7.724760×10^{9}	2.081019	0.538473
35	3.014847×10^{11}	2.081019	0.537089
40	1.176645×10^{13}	2.081019	0.536046
45	4.592252×10^{14}	2.081019	0.535233
50	1.792280×10^{16}	2.081019	0.534581
75	1.622957×10^{24}	2.081019	0.532615
100	1.469630×10^{32}	2.081019	0.531628
150	1.205065×10^{48}	2.081019	0.530637
200	9.881267×10^{63}	2.081019	0.530140
∞	∞	2.081019	0.528645

# of columns of hexagons=6			
n-1	K	q	κ
1	9.000000×10^{0}	4.500000	0.792481
2	2.000000×10^{1}	2.222222	0.617418
3	5.600000×10^{1}	2.800000	0.580735
4	1.690000×10^{2}	3.017857	0.569298
5	4.410000×10^{2}	2.609467	0.549040
6	1.258000×10^{3}	2.852608	0.541943
7	3.520000×10^{3}	2.798092	0.535516
8	9.701000×10^{3}	2.755966	0.529757
9	2.721600×10^{4}	2.805484	0.526149
10	7.572500×10^{4}	2.782371	0.522854
15	1.271586×10^{7}	2.786960	0.513046
20	2.135548×10^{9}	2.786438	0.508065
25	3.586882×10^{11}	2.786390	0.505052
30	6.024580×10^{13}	2.786390	0.503032
35	1.011897×10^{16}	2.786390	0.501584
40	1.699597×10^{18}	2.786390	0.500495
45	2.854668×10^{20}	2.786390	0.499646
50	4.794742×10^{22}	2.786390	0.498966
75	6.409340×10^{33}	2.786390	0.496919
100	8.567643×10^{44}	2.786390	0.495893
150	1.530938×10^{67}	2.786390	0.494864
200	2.735607×10^{89}	2.786390	0.494349
∞	∞	2.786390	0.492799

# of columns of hexagons=8			
n-1	K	q	κ
1	1.700000×10^{1}	8.500000	0.817493
2	4.900000×10^{1}	2.882353	0.623857
3	1.640000×10^{2}	3.346939	0.565966
4	7.690000×10^{2}	4.689024	0.563932
5	2.601000×10^{3}	3.382315	0.540231
6	9.826000×10^{3}	3.777778	0.530496
7	3.924900×10^{4}	3.994403	0.526220
8	1.429130×10^{5}	3.641188	0.518933
9	5.464480×10^{5}	3.823641	0.515128
10	2.092481×10^{6}	3.829241	0.512117
11	7.838417×10^{6}	3.745992	0.508936
12	2.984698×10^{7}	3.807781	0.506757
13	1.132814×10^{8}	3.795404	0.504818
14	4.280312×10^{8}	3.778479	0.503038
15	1.625161×10^{9}	3.796830	0.501606
20	1.270401×10^{12}	3.789581	0.496400
25	9.936482×10^{14}	3.789996	0.493265
30	7.771165×10^{17}	3.790101	0.491165
35	6.077653×10^{20}	3.790096	0.489660
40	4.753201×10^{23}	3.790095	0.488529
45	3.717376×10^{26}	3.790095	0.487649
50	2.907279×10^{29}	3.790095	0.486943
75	8.506254×10^{43}	3.790095	0.484822
100	2.488800×10^{58}	3.790095	0.483759
150	2.130557×10^{87}	3.790095	0.482694
200	1.823880×10^{116}	3.790095	0.482161
∞	∞	3.790095	0.480558

# of columns of hexagons=10			
n-1	K	q	κ
1	3.300000×10^{1}	16.500000	0.840732
2	1.250000×10^{2}	3.787879	0.633253
3	4.880000×10^{2}	3.904000	0.558171
4	3.653000×10^{3}	7.485656	0.563565
5	1.640100×10^{4}	4.489734	0.538519
6	7.959400×10^{4}	4.852997	0.525173
7	4.688750×10^{5}	5.890833	0.523301
8	2.273149×10^{6}	4.848092	0.515031
9	1.169150×10^{7}	5.143307	0.510412
10	6.324575×10^{7}	5.409548	0.508127
11	3.189763×10^{8}	5.043442	0.504444
12	1.658910×10^{9}	5.200732	0.502092
13	8.719050×10^{9}	5.255890	0.500326
14	4.475282×10^{10}	5.132763	0.498328
15	2.328376×10^{11}	5.202747	0.496849
20	8.770505×10^{14}	5.182546	0.491482
25	3.304532×10^{18}	5.189920	0.488247
30	1.244175×10^{22}	5.190122	0.486077
35	4.684541×10^{25}	5.189883	0.484523
40	1.763850×10^{29}	5.189890	0.483356
45	6.641333×10^{32}	5.189897	0.482448
50	2.500625×10^{36}	5.189897	0.481720
75	1.892413×10^{54}	5.189896	0.479533
100	1.432132×10^{72}	5.189896	0.478437
150	8.201960×10^{107}	5.189896	0.477340
200	4.697342×10^{143}	5.189896	0.476791
∞	∞	5.189896	0.475141

# of columns of hexagons=12			
n-1	K	q	κ
1	6.500000×10^{1}	32.500000	0.860338
2	3.240000×10^{2}	4.984615	0.641527
3	1.460000×10^{3}	4.506173	0.553250
4	1.775300×10^{4}	12.159589	0.564631
5	1.071850×10^{5}	6.037571	0.539024
6	6.537940×10^{5}	6.099678	0.522121
7	5.791824×10^{6}	8.858790	0.522455
8	3.774329×10^{7}	6.516650	0.513668
9	2.566096×10^{8}	6.798814	0.507909
10	1.999481×10^{9}	7.791917	0.506508
11	1.361217×10^{10}	6.807851	0.502450
12	9.589983×10^{10}	7.045156	0.499737
13	7.083335×10^{11}	7.386181	0.498299
14	4.939105×10^{12}	6.972853	0.496087
15	3.515425×10^{13}	7.117534	0.494492
20	6.505715×10^{17}	7.097110	0.489045
25	1.200526×10^{22}	7.133919	0.485736
30	2.210079×10^{26}	7.130499	0.483504
35	4.070403×10^{30}	7.128959	0.481910
40	7.497190×10^{34}	7.129329	0.480713
45	1.380847×10^{39}	7.129366	0.479781
50	2.543271×10^{43}	7.129342	0.479035
75	5.390528×10^{64}	7.129344	0.476793
100	1.142536×10^{86}	7.129344	0.475671
150	5.132713×10^{128}	7.129344	0.474547
200	2.305813×10^{171}	7.129344	0.473984
∞	∞	7.129344	0.472295

# of columns of hexagons=14			
n-1	K	q	κ
1	1.290000×10^{2}	64.500000	0.876403
2	8.450000×10^{2}	6.550388	0.648187
3	4.376000×10^{3}	5.178698	0.549791
4	8.746400×10^{4}	19.987203	0.566083
5	7.142730×10^{5}	8.166480	0.540170
6	5.400016×10^{6}	7.560157	0.520105
7	7.288210×10^{7}	13.496644	0.522381
8	6.432127×10^{8}	8.825387	0.513346
9	5.693587×10^{9}	8.851796	0.506355
10	6.479722×10^{10}	11.380736	0.505848
11	5.978731×10^{11}	9.226833	0.501552
12	5.644171×10^{12}	9.440417	0.498352
13	5.931721×10^{13}	10.509462	0.497321
14	5.624770×10^{14}	9.482527	0.494937
15	5.445216×10^{15}	9.680781	0.493150
16	5.512870×10^{16}	10.124244	0.492156
17	5.311365×10^{17}	9.634483	0.490682
18	5.189786×10^{18}	9.771098	0.489531
19	5.164227×10^{19}	9.950751	0.488695
20	5.019149×10^{20}	9.719071	0.487702
25	4.577406×10^{25}	9.837494	0.484334
30	4.151961×10^{30}	9.812572	0.482046
35	3.773012×10^{35}	9.807750	0.480420
40	3.428955×10^{40}	9.810614	0.479199
45	3.115766×10^{45}	9.810466	0.478248
50	2.831247×10^{50}	9.810266	0.477487
75	1.754105×10^{75}	9.810318	0.475200
100	1.086756×10^{100}	9.810317	0.474055
150	4.171432×10^{149}	9.810317	0.472909
200	1.601173×10^{199}	9.810317	0.472336
∞	∞	9.810317	0.470614

# of columns of hexagons=16			
n-1	K	q	κ
1	2.570000×10^{2}	128.500000	0.889514
2	2.209000×10^{3}	8.595331	0.653481
3	1.312400×10^{4}	5.941150	0.547197
4	4.346570×10^{5}	33.119247	0.567561
5	4.811297×10^{6}	11.069181	0.541414
6	4.470080×10^{7}	9.290801	0.518649
7	9.277822×10^{8}	20.755382	0.522618
8	1.114355×10^{10}	12.010954	0.513469
9	1.269413×10^{11}	11.391457	0.505279
10	2.131667×10^{12}	16.792543	0.505619
11	2.676416×10^{13}	12.555511	0.501184
12	3.350536×10^{14}	12.518742	0.497437
13	5.060426×10^{15}	15.103330	0.496840
14	6.538220×10^{16}	12.920297	0.494334
15	8.545805×10^{17}	13.070538	0.492297
16	1.222266×10^{19}	14.302520	0.491521
17	1.608466×10^{20}	13.159714	0.489958
18	2.143311×10^{21}	13.325182	0.488692
19	2.980831×10^{22}	13.907601	0.487962
20	3.967140×10^{23}	13.308839	0.486910
25	1.797383×10^{29}	13.611116	0.483492
30	8.062583×10^{34}	13.511832	0.481149
35	3.634844×10^{40}	13.503054	0.479498
40	1.638465×10^{46}	13.515825	0.478259
45	7.381906×10^{51}	13.513675	0.477292
50	3.326287×10^{57}	13.512821	0.476518
75	6.179189×10^{85}	13.513215	0.474195
100	1.147883×10^{114}	13.513214	0.473032
150	3.961232×10^{170}	13.513214	0.471868
200	1.366982×10^{227}	13.513214	0.471286
∞	∞	13.513214	0.469537

# of columns of hexagons=18			
n-1	K	q	κ
1	5.130000×10^{2}	256.500000	0.900282
2	5.780000×10^{3}	11.267057	0.657729
3	3.936800×10^{4}	6.811073	0.545169
4	2.172157×10^{6}	55.175701	0.568938
5	3.260269×10^{7}	15.009361	0.542576
6	3.703665×10^{8}	11.359999	0.517534
7	1.190319×10^{10}	32.138956	0.522979
8	1.951311×10^{11}	16.393171	0.513776
9	2.836579×10^{12}	14.536785	0.504479
10	7.082512×10^{13}	24.968503	0.505597
11	1.213984×10^{15}	17.140588	0.501087
12	1.997523×10^{16}	16.454273	0.496780
13	4.370140×10^{17}	21.877797	0.496614
14	7.710267×10^{18}	17.643068	0.494027
15	1.350612×10^{20}	17.517053	0.491707
16	2.749012×10^{21}	20.353832	0.491168
17	4.946276×10^{22}	17.992921	0.489537
18	8.940841×10^{23}	18.075906	0.488127
19	1.748606×10^{25}	19.557512	0.487526
20	3.187554×10^{26}	18.229116	0.486423
25	7.196387×10^{32}	18.899692	0.482960
30	1.598731×10^{39}	18.601520	0.480561
35	3.590070×10^{45}	18.595996	0.478895
40	8.054217×10^{51}	18.638150	0.477640
45	1.804779×10^{58}	18.626520	0.476659
50	4.046068×10^{64}	18.624162	0.475876
75	2.291018×10^{96}	18.625993	0.473522
100	1.297206×10^{128}	18.625984	0.472344
150	4.158820×10^{191}	18.625984	0.471165
200	1.333310×10^{255}	18.625984	0.470576
∞	∞	18.625984	0.468805

# of columns of hexagons=20			
n-1	K	q	κ
1	1.025000×10^{3}	512.500000	0.909219
2	1.512900×10^{4}	14.760000	0.661192
3	1.181000×10^{5}	7.806200	0.543537
4	1.089456×10^{7}	92.248611	0.570173
5	2.216634×10^{8}	20.346247	0.543604
6	3.069817×10^{9}	13.848999	0.516648
7	1.535594×10^{11}	50.022325	0.523380
8	3.440876×10^{12}	22.407461	0.514147
9	6.345282×10^{13}	18.440892	0.503854
10	2.369650×10^{15}	37.345069	0.505679
11	5.558039×10^{16}	23.455107	0.501130
12	1.193520×10^{18}	21.473754	0.496280
13	3.806281×10^{19}	31.891233	0.496527
14	9.188878×10^{20}	24.141352	0.493890
15	2.142779×10^{22}	23.319270	0.491271
16	6.245128×10^{23}	29.144989	0.490976
17	1.538323×10^{25}	24.632374	0.489296
18	3.751489×10^{26}	24.386870	0.487722
19	1.037499×10^{28}	27.655664	0.487262
20	2.591953×10^{29}	24.982697	0.486119
21	6.475988×10^{30}	24.984979	0.485085
22	1.736763×10^{32}	26.818500	0.484607
23	4.381100×10^{33}	25.225666	0.483788
24	1.108992×10^{35}	25.313091	0.483057
25	2.921041×10^{36}	26.339607	0.482613
30	3.214192×10^{43}	25.584864	0.480157
35	3.607181×10^{50}	25.611311	0.478482
40	4.037345×10^{57}	25.726338	0.477215
45	4.508126×10^{64}	25.682821	0.476222
50	5.040105×10^{71}	25.678457	0.475430
75	8.797124×10^{106}	25.684759	0.473051
100	1.535370×10^{142}	25.684723	0.471861
150	4.676890×10^{212}	25.684723	0.470669
200	1.424628×10^{283}	25.684723	0.470073
∞	∞	25.684723	0.468284

# of columns of hexagons=22			
n-1	K	q	κ
1	2.049000×10^{3}	1024.500000	0.916725
2	3.960500×10^{4}	19.328941	0.664061
3	3.542960×10^{5}	8.945739	0.542194
4	5.477073×10^{7}	154.590311	0.571264
5	1.509902×10^{9}	27.567680	0.544497
6	2.544848×10^{10}	16.854393	0.515923
7	1.988914×10^{12}	78.154511	0.523784
8	6.095655×10^{13}	30.648165	0.514526
9	1.420142×10^{15}	23.297605	0.503350
10	7.969044×10^{16}	56.114432	0.505813
11	2.561750×10^{18}	32.146265	0.501245
12	7.139607×10^{19}	27.870037	0.495883
13	3.335857×10^{21}	46.723252	0.496518
14	1.103800×10^{23}	33.088952	0.493850
15	3.406923×10^{24}	30.865399	0.490932
16	1.429171×10^{26}	41.949020	0.490877
17	4.825645×10^{27}	33.765349	0.489164
18	1.579541×10^{29}	32.732219	0.487414
19	6.207337×10^{30}	39.298371	0.487104
20	2.126923×10^{32}	34.264658	0.485930
21	7.201585×10^{33}	33.859172	0.484793
22	2.719177×10^{35}	37.758034	0.484406
23	9.416014×10^{36}	34.628179	0.483561
24	3.250934×10^{38}	34.525581	0.482770
25	1.197678×10^{40}	36.841058	0.482382
30	6.522925×10^{47}	35.138596	0.479867
35	3.669683×10^{55}	35.271860	0.478191
40	2.052626×10^{63}	35.547390	0.476914
45	1.143393×10^{71}	35.416202	0.475908
50	6.386354×10^{78}	35.412289	0.475110
75	3.463814×10^{117}	35.430011	0.472709
100	1.878511×10^{156}	35.429936	0.471508
150	5.524971×10^{233}	35.429933	0.470306
∞	∞	35.429933	0.467900

# of columns of hexagons=24			
n-1	K	q	κ
1	4.097000×10^{3}	2048.500000	0.923104
2	1.036840×10^{5}	25.307298	0.666473
3	1.062884×10^{6}	10.251186	0.541069
4	2.757703×10^{8}	259.454767	0.572222
5	1.029586×10^{10}	37.334922	0.545268
6	2.109795×10^{11}	20.491674	0.515319
7	2.583514×10^{13}	122.453315	0.524169
8	1.083195×10^{15}	41.927195	0.514889
9	3.179234×10^{16}	29.350530	0.502931
10	2.690344×10^{18}	84.622382	0.505971
11	1.186464×10^{20}	44.100831	0.501393
12	4.273574×10^{21}	36.019415	0.495558
13	2.937360×10^{23}	68.733097	0.496553
14	1.333907×10^{25}	45.411757	0.493869
15	5.423545×10^{26}	40.659104	0.490659
16	3.288725×10^{28}	60.637921	0.490837
17	1.523958×10^{30}	46.338865	0.489101
18	6.664425×10^{31}	43.731034	0.487172
19	3.737358×10^{33}	56.079228	0.487012
20	1.757849×10^{35}	47.034525	0.485814
21	8.033464×10^{36}	45.700544	0.484567
22	4.287331×10^{38}	53.368400	0.484277
23	2.038992×10^{40}	47.558549	0.483411
24	9.570391×10^{41}	46.936867	0.482552
25	4.948532×10^{43}	51.706682	0.482226
30	1.332398×10^{52}	48.171337	0.479652
35	3.768472×10^{60}	48.573939	0.477980
40	1.054733×10^{69}	49.174846	0.476694
45	2.932597×10^{77}	48.832901	0.475676
50	8.195459×10^{85}	48.841199	0.474873
75	1.389501×10^{128}	48.884326	0.472454
100	2.355597×10^{170}	48.884337	0.471244
150	6.769817×10^{254}	48.884314	0.470033
∞	∞	48.884314	0.467608

# of columns of hexagons=26			
n-1	K	q	κ
1	8.193000×10^{3}	4096.500000	0.928584
2	2.714450×10^{5}	33.131332	0.668530
3	3.188648×10^{6}	11.746940	0.540113
4	1.389866×10^{9}	435.879504	0.573062
5	7.024849×10^{10}	50.543346	0.545936
6	1.749165×10^{12}	24.899679	0.514808
7	3.362949×10^{14}	192.260256	0.524530
8	1.928783×10^{16}	57.353906	0.515224
9	7.118159×10^{17}	36.904930	0.502579
10	9.109545×10^{19}	127.976133	0.506138
11	5.514436×10^{21}	60.534700	0.501553
12	2.558916×10^{23}	46.403945	0.495286
13	2.595923×10^{25}	101.446207	0.496614
14	1.619401×10^{27}	62.382496	0.493921
15	8.640019×10^{28}	53.353161	0.490434
16	7.600362×10^{30}	87.966965	0.490832
17	4.838195×10^{32}	63.657420	0.489082
18	2.815439×10^{34}	58.191939	0.486974
19	2.261281×10^{36}	80.317175	0.486962
20	1.461149×10^{38}	64.615969	0.485749
21	8.979245×10^{39}	61.453323	0.484386
22	6.796967×10^{41}	75.696419	0.484195
23	4.442067×10^{43}	65.353664	0.483314
24	2.825341×10^{45}	63.604202	0.482381
25	2.056916×10^{47}	72.802407	0.482120
30	2.734036×10^{56}	65.901714	0.479486
35	3.898427×10^{65}	66.891242	0.477825
40	5.464586×10^{74}	68.113143	0.476531
45	7.584862×10^{83}	67.310739	0.475500
50	1.061972×10^{93}	67.365370	0.474694
75	5.653762×10^{138}	67.459521	0.472260
100	3.009870×10^{184}	67.460373	0.471041
150	8.529897×10^{275}	67.460248	0.469822
∞	∞	67.460248	0.467382

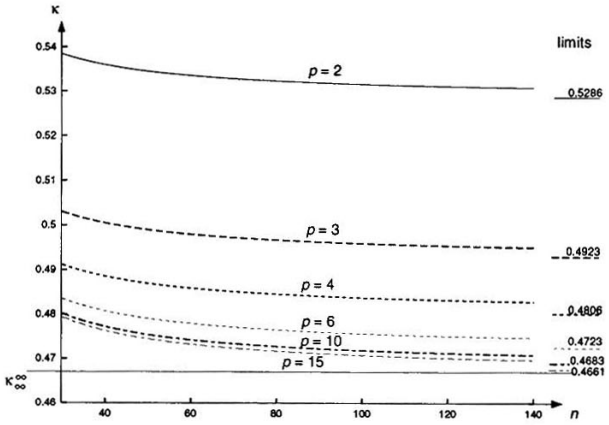

Figure 23a.

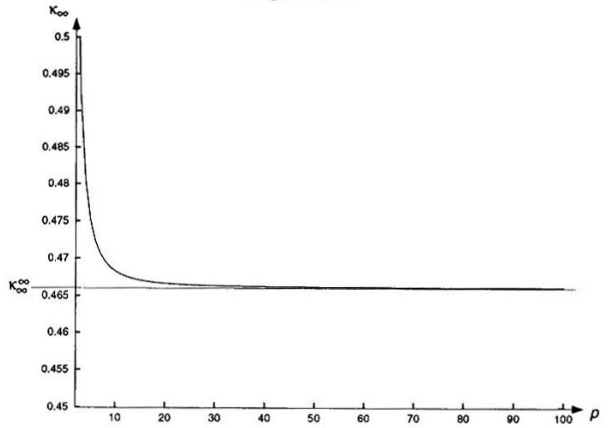

Figure 23b.

References

[1] S. Iijima, Helical Microtubules of Graphitic Carbon, *Nature* 354 (1991) 56-58.

[2] J. W. Mintmire, B. I. Dunlap and C. T. White, Are Fullerene Tubules Metallic? *Physical Review letters*, 68 (1992) 631-634.

[3] T. W. Ebbesen and P. M. Ajayan, Large-scale Synthesis of Carbon Nanotubes, *Nature*, 358 (1992) 220 - 222.

[4] N. Hamada, S. Sawada and A. Oshiyama, New One-dimensional Conductor: Graphitic Microtubules, *Physical Review Letters*, 68 (1992) 1579-1581.

[5] P. M. Ajayan and S. Iijima, Capillarity-induced Filling of Carbon Nanotubes, *Nature*, 361 (1993) 333-334.

[6] P. M. Ajayan and S. Iijima, Smallest Carbon Nanotube Scientific Correspondence, *Nature*, 358 (1992) 23.

[7] S. Iijima, T. Ichihashi and Y. Ando, Pentagons, Heptagons and Negative Curvature in Graphite Microtubule Growth, *Nature*, 356 (1992) 776-778.

[8] J. Maddox, Calculating the Energy of Fullerenes, *Nature*, 363 (1993) 395.

[9] S. Iijima and T. Ichihashi, Single-shell Carbon Nanotubes of 1-nm diameter, *Nature* 363 (1993) 603-605.

[10] P. W. Fowler, Cylindrical Fullerenes: the Smallest Nanotubes? *Journal of the Physics and Chemistry of Solid*, 54 (1993) 1825-1833.

[11] X. Lin, X. K. Wong, V. P. Dravid, R. P. H. Chang and J. B. Ketterson, Large Scale Synthesis of Single-shell Carbon Nanotubes, *Applied Physics Letters*, 64 (1994) 181-183.

[12] S. Iijima, P. M. Ajayan and T. Ichihashi, Growth Model for Carbon Nanotubes, *Physical Review Letters*, 69 (1992) 3100-3103.

[13] C. H. Kiang, W. A. Goddard, R. Beyers and D. S. Bethune, Growth and Properties of Single-shell Carbon Nanotubes, *Abstract of Papers of the American Chemical Society*, 207 (1994), Mar 13.

[14] R. Swinborne - Sheldrake, W. C. Herndon and I. Gutman, Kekulé Structures and Resonance Energies of Benzenoid Hydrocarbons, *Tetrahedron Letters*, 10 (1975) 755-758.

[15] W. A. Seitz, D. J. Klein, T. G. Schmalz and M. A. Garcia-Bach, The Poly-polyacene Family of Multi-face π-network Polymers in a Valence-bond Picture, *Chemical Physics Letters*, 115 (1985) 139-143.

[16] S. J. Cyvin and I. Gutman, Kekulé Structures in Benzenoid Hydrocarbons, *Lecture Notes in Chemistry* 46, Springer-Verlag, Berlin, Heidelberg, New York, 1988.

[17] M. Gordon and W. H. T. Davison, Theory of Resonance Topology of Fully Aromatic Hydrocarbons, *Journal of Chemical Physics*, 20 (1952) 428-435.

[18] P. W. Kasteleyn, The Statistics of Dimers on a Lattice I. The Number of Dimer Arrangements on a Quadratic Lattice, *Physica*, 27 (1961) 1209-1225.

[19] P. W. Kasteleyn, Graph Theory and Crystal Physics, In: Graph Theory and Theoretical Physics (Ed. F. Harray), Academic Press London 1967, pp. 43 - 110.

[20] K. Al-Khnaifes and H. Sachs, Graphs, Linear Equations, Determinants, and the Number of Perfect Matchings, In: Contemporary Methods in Graph Theory (Ed. R. Bodendiek), B. I. - Wissenschaftsverlag Mannheim - Wien - Zürich, 1990, pp. 47-71.

[21] P. John and H. Sachs, Calculating the Numbers of Perfect Matchings and of Spanning Trees, Pauling's Orders, the Characteristic Polynomial, and the Eigenvectors of a Benzenoid System, In: Advances in the Theory of Benzenoid Hydrocarbons (Ed. I. Gutman and S. J. Cyvin), *Topics in Current Chemistry*, 153 (1990) 145-179.

[22] P. John and H. Sachs, Calculating the Characteristic Polynomial, Eigenvectors and Number of Spanning Trees of a Hexagonal System, *Journal of Chemical Society Faraday Transactions*, 86 (1990) 1033-1039.

[23] P. J. Davis, Circulant Matrices, John Wiley & Sons, New York, Chichester, Brisbane, Toronto, 1979.